# 1 Independent particle model

In classical mechanics, a system of particles of mass $M$ which interact through a two-body force (particle-particle potential) of the type shown in Fig. 1.1, that is described by the Hamiltonian

$$H = \frac{p^2}{2m} + v(r_{12}), \tag{1.1}$$

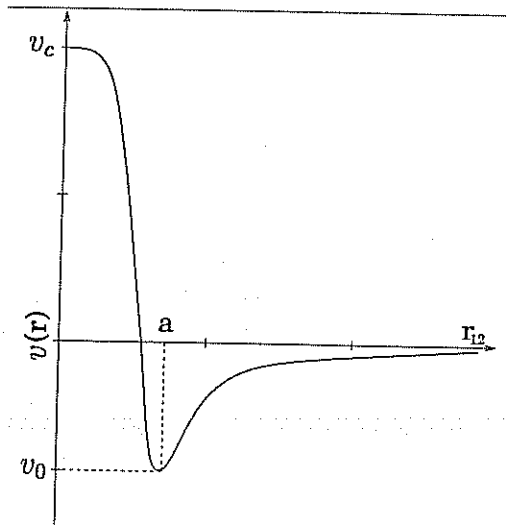


Fig. 1.1. Schematic representation of a two-body force acting among a system of particles, displayed as a function of the relative particle-particle coordinate $r_{12} = |\vec{r_1} - \vec{r_2}|$. It displays a repulsive core at $r_{12} = 0$ of strength $v_c$ and an attractive minimum of strengh $v_0$ at $r_{12} = a$.

will find the lowest state at zero temperature, by minimizing, for each particle,

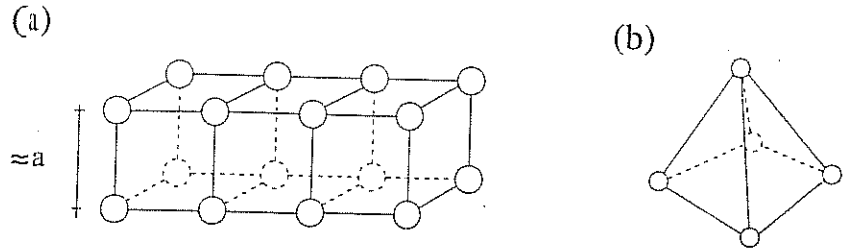


Fig. 1.2. Examples of the state of minimum energy of a system of classical particles described by the Hamiltonian given in Eq.(1.1).

its potential energy with respect to all its neighbours. Such static, localized particles, provide the basic design for the ground state of molecules and crystals (Fig. 1.2). While the laws governing the motion of these particles are invariant with respect to translation, in particular $v(r_{12})$, the solution of such equations violate translational and/or rotational invariance (cf. Fig. 1.2). In other words, the solution of the classical equations may display a lower symmetry than the original Hamiltonian. This phenomenon, known as *spontaneous symmetry breaking*, is perfectly allowed in classical mechanics and is at the basis of the *emergent properties* of the system of particles described by the Hamiltonian given in Eq.(1.1). In fact, the system in Fig. 1.2(a) will display localization and rigidity, *properties not contained in each individual particle, nor in H* [19].

In quantum mechanics

$$\Delta_x \Delta_p \geq \hbar. \tag{1.2}$$

Consequently, the (zero point) energy associated with the localization of a particle within a volume of radius $a$ is $\sim \hbar^2/Ma^2$. Thus, the particles described by the Hamiltonian given in Eq.(1.1) may be delocalized because the potential energy gain of the classical (localized) configuration may be overwhelmed by the quantal zero point energy. Consequently, systems for which the "quantality" parameter (at zero temperature) (cf. App. R)

$$Q = \frac{\text{zero point energy of localization}}{\text{potential energy of localization}} \approx \frac{\hbar^2}{ma^2}\frac{1}{|v_0|} \tag{1.3}$$

is $Q \ll 1$ are expected to display particle localization, while systems associated with larger values of $Q$ are expected to display particle delocalization. In the case of nucleons ($^1S_0$ nucleon-nucleon potential), $v_0 = -100$MeV, $a \approx 1$fm, $\hbar^2/M \approx 40$MeVfm$^2$ ($m = M \approx 10^3$MeV) and $Q = 0.4$ [20]. It is thus expected that nucleons, inside the nucleus, are delocalized [21].

Because nucleons do not occupy all the space available to them but are self confined, it is said that the nucleus is a quantum liquid. This is not completely correct, in the sense that the nucleus, as we shall see below, behaves

like caoutchouc, that is, the rubber of which tires of cars are made of, or like Fun Zone (micronite), a fad toy among youngsters. It deformes plastically under strain (cf. Ch. 16) and it reacts elastically to an instantaneous sollicitation (cf. Ch. 5).

In the case where the particles under consideration are $Ne_{20}$ atoms, $m = 20M$, $a \approx 3.1$Å and $v_0 = 3.1$meV. Consequently, $Q \approx 0.007$ and $N_{20}$ is, at $T = 0$ a solid, being a gas at room temperature.

Let us conclude these introductory remarks by noting that the results discussed above (namely that $Q \ll 1$ implies localization and thus spontaneous symmetry breaking, while $Q \sim 1$ does not), is an example of the fact that while *potential energy always prefers special arrangements, fluctuations, quantum or classical, favour symmetry.*

# 2
# Mean field

Because $Q$ is of order of 1 in the nuclear case, it is likely that mean field theory is applicable to the description of the motion of the nucleons. The marked variation of the binding energy per particle as a function of mass number $A = N + Z$ (cf. Fig. 2.1) (where $N$ and $Z$ stand for the number of neutrons and protons respectively), for specific values of $N$ and of $Z$ (magic numbers), testifies to the fact that nucleons in the nucleus display a long mean free path (in states close to the Fermi energy (cf. Ch. 4)).

Special stability is adscribed to nuclei displaying particular values of $N$ and $Z$ (*magic numbers*). In particular to ${}^{208}_{82}Pb_{126}$ containing 82 protons and 126 neutrons. In analogy with the atomic case in general, and with the noble gases in particular, this result is connected with the filling of shells, single-particle orbitals of a single-particle potential $U(r)$ generated by all the nucleons, and where each nucleon move independently. The validity of the independent-particle model implies that the *matrix elements of* $U(r)$ *are much larger than those of* $(v(r_{12}) - U(r))$. In other words, that

$$H_{MF} = T + U(r) \tag{2.1}$$

is a good approximation to Eq. (1.1) (i.e. $H = T + U - (v - U) \approx T + U$).

Nucleon-nucleus elastic scattering data, and one-particle stripping and pick-up experiments (cf. Figs. 2.2 and 2.3) provide the information needed to determine the parameter describing $U(r)$, and the energy and occupation probability of single-particle states.

The properties of the single-particle levels close to $E = |\varepsilon - \varepsilon_F| < 5\text{MeV}$ (valence levels) can be quite accurately described making use of a single-particle Saxon-Woods potential (a spin-orbit and a Coulomb term has to be added),

$$U(r) = \frac{U}{1 + \exp\left(\frac{r - R_0}{a}\right)}, \tag{2.2}$$

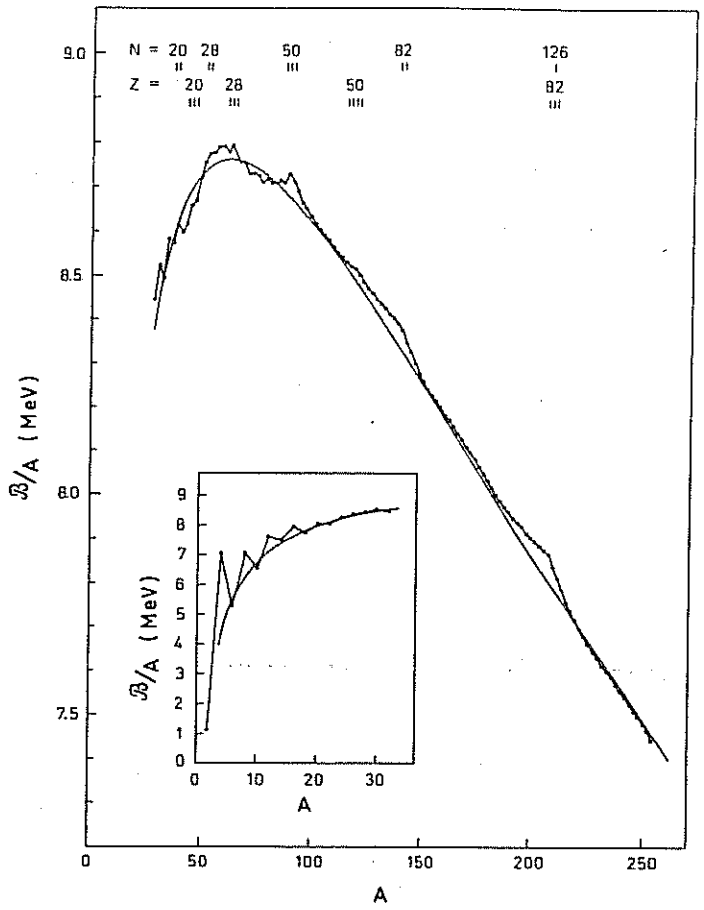


Fig. 2.1. Binding energy per nucleon as a function of mass number (after ref. [22]).

where $R_0 = 1.2A^{1/3}$fm is the nuclear radius and $a = 0.65$ fm the diffusivity of the potential, while the relation

$$U = U_0 + V_1 \frac{N-Z}{A} \tau_z. \tag{2.3}$$

defines the depth of the potential, with $U_0 = -45, -50$MeV. To describe the centroid of levels with $E >$ 5MeV – 10MeV, a term $0.3E$ has to be added to $U$, where $E = |\varepsilon - \varepsilon_F|$ is the absolute value of the single-particle measured from the Fermi energy. In other words, the depth of the empirical Saxon-Woods potential is

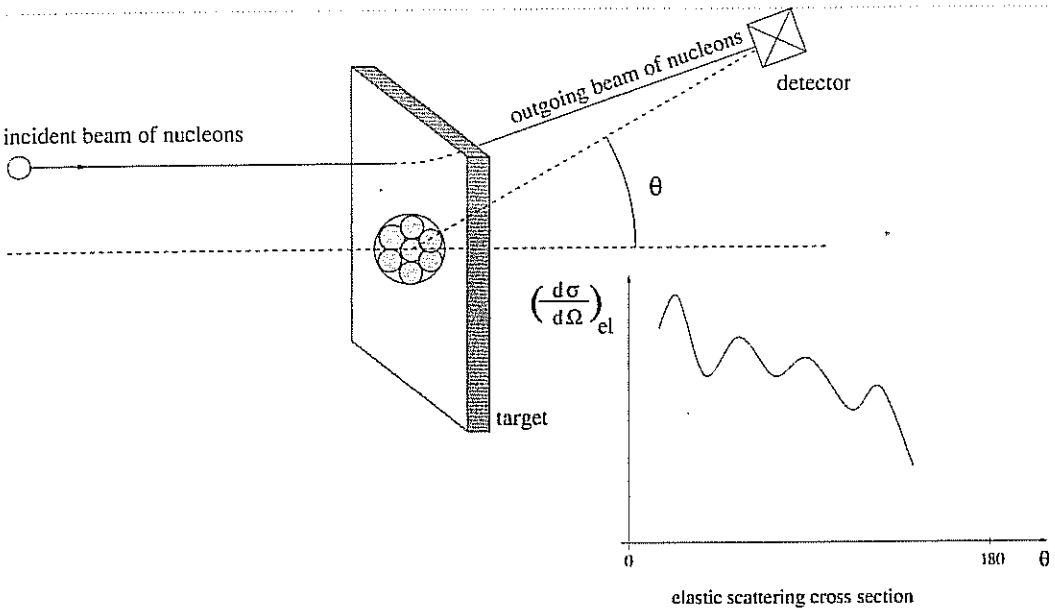


Fig. 2.2. Schematic representation of nucleon-nucleus elastic scattering.

$$\begin{aligned} U \quad & ( \quad E < 5\text{MeV}), \\ U + 0.3E \quad & ( \quad E > 5 - 10\text{MeV}). \end{aligned} \tag{2.4}$$

The last term in Eq. (2.3) is closely related to the symmetry energy in the nuclear mass formula of Weizäcker $V_1 = 30$MeV and $\tau_Z = +1$ for neutrons and $\tau_F = -1$ for protons. This term expresses the fact that one has to pay a prize to separate protons from neutrons (cf. e.g. Eq(5.8)), or to have a system with a neutron excess, needed in order to decrease Coulomb repulsion among protons.

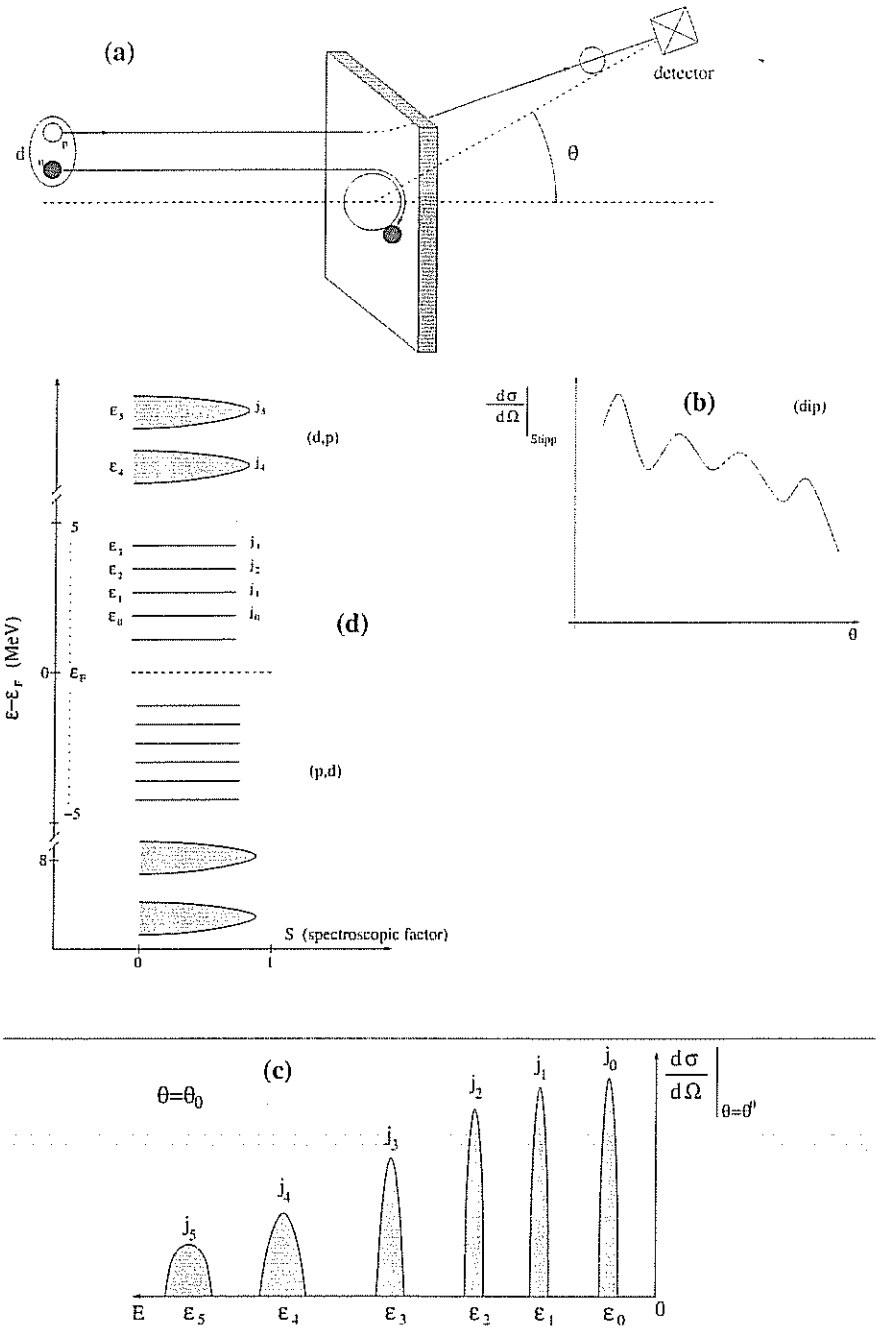


Fig. 2.3. Schematic representation of one-particle stripping reaction. The resulting cross section (b) are displayed in (c) for a given angle. The spectrum resulting from stripping and from pick-up reactions is shown in (d).

## 2.1 Hartree theory

Mean field theory in the version first proposed by *Hartree* finds that *the energy of the system acquires a minimum* by placing the nucleons in the potential

$$U_H(r) = \int \mathrm{d}^3 r' \rho(r') v(|\vec{r} - \vec{r'}|), \tag{2.5}$$

where

$$\rho(r) = \sum_{i \in \mathrm{occ}} |\varphi_i(\vec{r})|^2, \tag{2.6}$$

is the density of the system, sum of the modulus squared of the single-particle wavefunctions, solution of the Schrödinger equation

$$\begin{aligned} & \left(-\frac{\hbar^2}{2m}\nabla_r^2 + U_H(r)\right)\varphi_j(\vec{r}), \\ = & -\frac{\hbar^2}{2m}\nabla_r^2\varphi_j(r) + \sum_{i \in \mathrm{occ}} \int \mathrm{d}^3 r' \varphi_i^*(\vec{r'}) v(|\vec{r} - \vec{r'}|)\varphi_i(\vec{r'})\varphi_j(\vec{r}), \\ = & \varepsilon_j \varphi_j(\vec{r}). \end{aligned} \tag{2.7}$$

The sum in Eq. (2.6) is over all the occupied states, while $v(|\vec{r} - \vec{r'}|)$ is the nucleon-nucleon potential (two-body interaction, cf. Fig.1.1). The Hartree potential $U(r)$ reproduces rather well the main features of the empirical Saxon-Woods potential.

Equations (2.6-15.9) are self-consistent partial differential equation, to be solved by iteration starting from an ansatz for $U(r)$ (e.g. square well potential). With such a potential one can calculate a set of wavefunctions $\varphi_j$ which can be used to calculate the potential to be used in the next step of the iteration. Eventually, the solutions of this set of equations after a few steps, converge, that is, the input wavefunctions and resulting energies are reproduced by the calculated potential . This is because Hartree theory emerges from an *argument of minimization* (cf. Appendix B).

## 2.2 Constrained Hartree theory

To be noted that in solving Eqs. (2.5-~~15.9~~), one has to specify the *shape of the system*. For example whether the system is expected to be spherical or deformed. That is, Hartree theory is always *constrained Hartree theory*, in the sense that one looks for a minimum of energy for the particles moving in a potential whose density is either spherical symmetric or behaves as a tensor of rang $L$. To be noted that not all shape constrains lead to a self-consistent solution.

For a closed shell system, it is quite natural that the *absolute minimum* of the system is *spherical* (cf. Fig. 2.4(a)), while a system with a number of nucleons outside closed shell will deform under the polarization effect of these nucleons, like the moon and the sun polarize the earth (Jahn-Teller effect, cf. Fig. 2.4(b)). In this case and assuming a quadrupole, axial symmetric deformation [22],

$$R = R_0(1 + \beta_2 Y_{20}(\theta, \phi)), \tag{2.8}$$

is the radius of the Saxon-Woods potential and the system defines a privileged direction in space, violating rotational invariance, in spite of the fact that all nucleons, as well as the Hamiltonian introduced in Eq.(1.1) are invariant with respect to rotations. This again is an example of the phenomenon of *spontaneous symmetry breaking*.

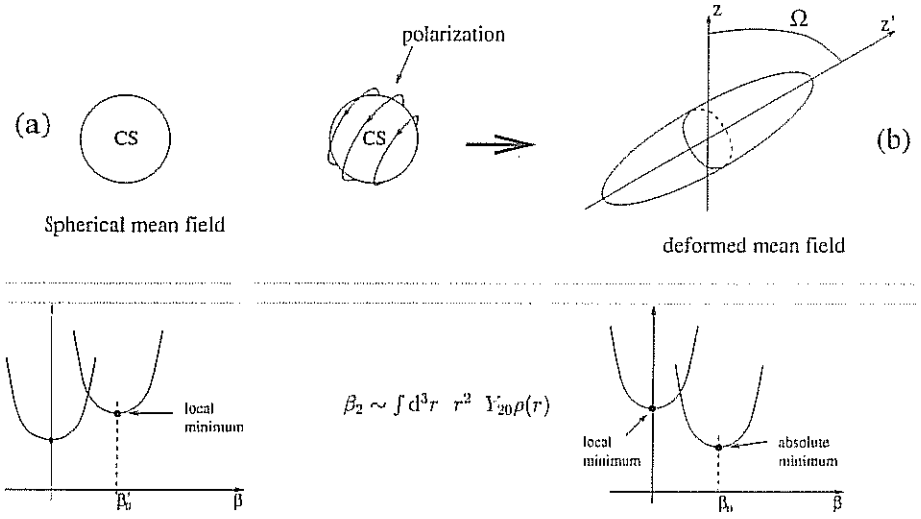


Fig. 2.4.

The ground state wavefunction, resulting from the filling of the lowest single-particle orbits of the deformed Saxon-Woods [5] potential (Eqs. (2.2),(2.3) and (2.8)), can be written as

$$\Phi_0 = \prod_{i=1}^{A} \varphi_{\nu_i}(\vec{r}_i). \tag{2.9}$$

It is a wavepacket of different angular momenta, being associated with fixed values of the Euler angles Ω (Fig. 2.4(b)), that is,

$$\Phi_0(\Omega) = \sum_I c_I \Psi_I \tag{2.10}$$

It can be shown (cf. Chs. 11 and 13) that there is a term in the residual interaction $(v - U)$ which has been neglected in $H_{MF}$, which leads to zero point fluctuations in the orientation of the system, which once taken into account, leads to solutions of $H$ which transform in an irreducible way with respect to rotations, that is,

$$\Phi_{IMK}(\vec{r_1} \ldots \vec{r_A}) \sim \int \mathrm{d}\Omega \mathcal{D}^{I*}_{MK}(\Omega)\Phi_0(\Omega; \vec{r_1} \ldots \vec{r_A}). \tag{2.11}$$

Here, $\mathcal{D}^{I}_{MK}(\Omega)$ is a rotational matrix, $\Omega \sim (\theta, \phi, \psi)$ the corresponding Euler angles, $K$ and $M$ being the projection of the total angular momentum $I$ on the intrinsic axis $z'$ fixed to the body and on the laboratory axis $z$ respectively (cf. Fig. 2.5).

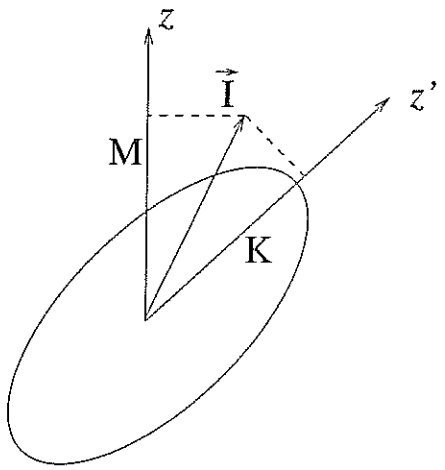


Fig. 2.5. .

The states $|IMK\rangle$ are the members of a rotational band (Fig. 2.6) associated with the different, quantized, frequencies of rotation.

The mean field solutions $\Psi_{IMK}$ fulfills the requirement that the eigenfunctions of a Hamiltonian which is invariant with respect to a group of symmetry (rotation group in the present case), should transform according to the irreducible representations of this group, that is they must behave as a tensor with respect to rotations.

From a mathematical point of view one can say that being $\Omega$ and $I$ conjugate variables, one can choose which one to conserve in working out the solution of the problem (cf. App. U). In the present case, it turns out that it is simpler to solve the problem in a representation in which $\Omega$ has a fixed value (and consequently $I$ is completely indefinite, $\Delta\Omega\Delta I \geq \hbar$). Once this solution is found one can, through a change of representation (Fourier transform), go to the representation in which $I$ is a good quantum number. This is precisely what is

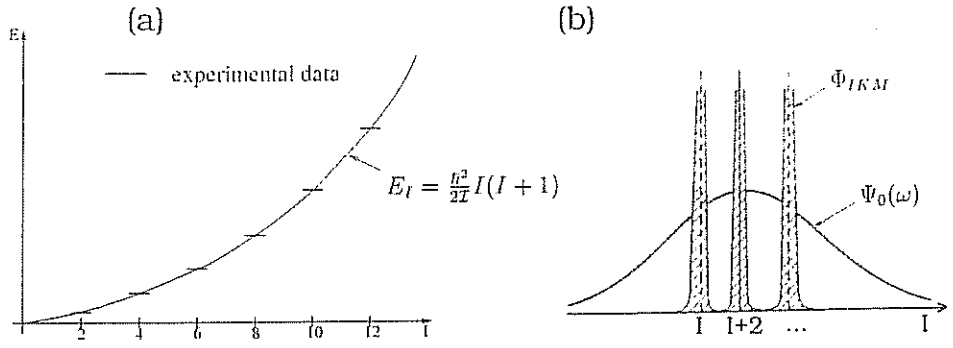


Fig. 2.6. .

accomplished through the integral (projection) given in Eq. (2.11), a projection which is equivalent to

$$\Phi_{IMK} \sim \int d\Omega e^{-i\vec{\Omega}.\vec{I}} \Phi_0(\Omega), \tag{2.12}$$

in keeping with the fact that

$$\mathcal{D}^I_{MK}(\Omega) = \langle IK|\exp(-i\vec{\Omega}.\vec{I})|IM\rangle, \tag{2.13}$$

the operator

$$\mathcal{R}(\Omega) = e^{-i\vec{\Omega}.\vec{I}},$$

generating a general rotation in space.

In the description of many-body systems having a shape deviating from spherical symmetry (nonspherical nuclei, molecules, etc.), it is convenient to employ an intrinsic (or body-fixed) coordinate frame (Fig. 2.7). The transformation of operators from the fixed frame (the laboratory system), to the intrinsic frame involves special features as a result of the fact that the orientation angles of the intrinsic frame, are to be regarded as dynamical variables [22]. The states of orientation can be specified by the angular variables or by the associated angular momenta.

In fact, the state of orientation of the body-fixed system is completely specified by the three angular momentum quantum numbers $IKM$ representing the conjugate variables of the three orientation angles $\Omega = (\phi, \theta, \psi)$.

The state $|\Omega\rangle$ with orientation $\Omega$ with respect to $\mathcal{K}$ has the orientation $\Omega = 0$ with respect to $\mathcal{K}'$, that is

$$|\Omega = 0\rangle_{\mathcal{K}'} = |\Omega\rangle_{\mathcal{K}},$$

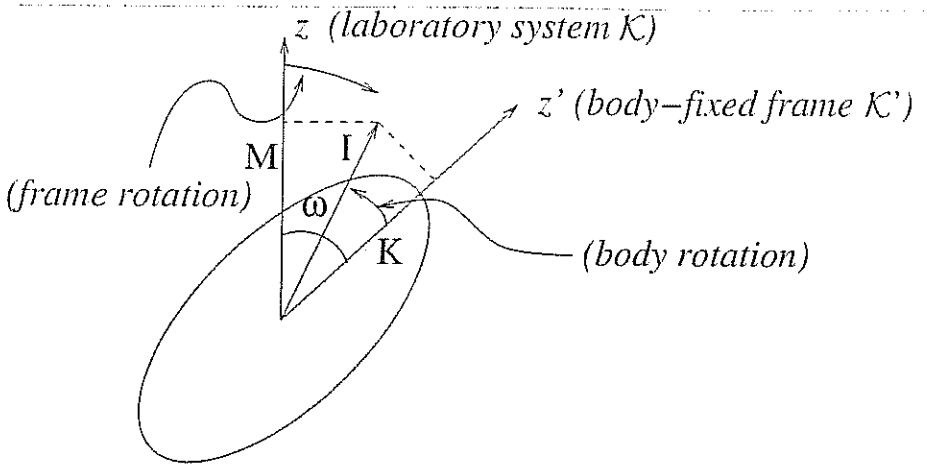


Fig. 2.7.

where

$$|IKM\rangle_{\mathcal{K}'} = \mathcal{R}(\Omega)|IKM\rangle_{\mathcal{K}},$$

and

$$\mathcal{R}(\Omega) = e^{-i\vec{\Omega}.\vec{I}},$$

leading to a rotation of the coordinate system.

### 2.3 Hartree-Fock theory

Because nucleons are fermions, the product $\varphi_i(\vec{r'})\varphi_j(\vec{r})$ appearing in Eq.(15.9) has to be replaced by the antisymmetric product $\varphi_i(\vec{r'})\varphi_j(\vec{r}) - \varphi_i(\vec{r})\varphi_j(\vec{r'})$. In this way, a particle does not interact with itself (note that in Eqs.(2.5) and (2.6) all particles, including the nucleon in question, contribute to the mean field potential felt by a given nucleon), and all fermions become indistinguishible. By the same token, the state $\Phi_0$ (Eq.(2.9)) becomes

$$\Phi_0 = \frac{1}{\sqrt{A!}}\det\left[\varphi_{\nu_1}(\vec{r_1})\ldots\varphi_{\nu_N}(\vec{r_N})\right], \tag{2.14}$$

that is, a normalized determinant, and Eq.(15.9) can be written as

$$\left[-\frac{\hbar^2}{2m}\nabla_r^2 + U_H(r)\right]\varphi_j(\vec{r}) + \int \mathrm{d}^3r' U_x(\vec{r},\vec{r'})\varphi_j(\vec{r'}) = \varepsilon_j\varphi_j(\vec{r}), \tag{2.15}$$

where the non-local potential

$$U_x(\vec{r},\vec{r'}) = -\sum_{i\in \text{occ}} \varphi_i^*(\vec{r'})v(|\vec{r}-\vec{r'}|)\varphi_i(\vec{r}), \tag{2.16}$$

is the so called exchange or Fock potential.

Equation (2.15) together with Eqs.(2.5), (2.6) and(2.16) are the integro-differential self-consistent equations known as Hartree-Fock equations.

Hartree-Fock theory provides a potential in which all particles can be accomodated, *or packed, in such an efficient way* so as that all levels are fully occupied up to the highest level (Fermi energy $\varepsilon_F$) and empty from there on, leading to a density (Eq. (2.6)) which generates the same potential weighted with the two-body interaction (Eqs. (2.6) and (2.16)). In other words, at equilibrium the system of particles displays a self-consistent relation between density $\rho(r)$ and potential $U(r)$, mediated by the two-body interaction $v(|\vec{r}-\vec{r'}|)$.

It is, as a rule, not simple to deal numerically with non-local potential. There are a number of ways in which one can make local $U_x$. In particular in terms of the so called $k$-mass [7]. In fact, for most purposes the effect of the term containing $U_x$ in Eq.(2.15) can be taken into account by replacing $m$ in the kinetic energy term by (cf. App. C)

$$m_k = m\left(1+\frac{m}{\hbar^2 k}\frac{\partial \widetilde{U_x}}{\partial k}\right)^{-1}, \tag{2.17}$$

where $\widetilde{U_x}(k)$ is the Fourier transorm of the exchange potential. Making use of Eq.(2.3) and of the fact that $E = \frac{\hbar^2}{2m}|k^2 - k_F^2|$, one obtains

$$m_k \approx 0.7m. \tag{2.18}$$

The (local) equation

$$\left(-\frac{\hbar^2}{2m_k}\nabla_r^2 + U'(r)\right)\varphi_j(\vec{r}) = \varepsilon_j\varphi_j(\vec{r}) \tag{2.19}$$

with $U'(r) = \frac{m}{m_k}U_H(r)$, leads to a set of levels which display the following properties:

1) the sequence of levels essentially coincides with whose observed experimentally,

2) the density of levels coincide also with that observed experimentally for single particle states with $E = |\varepsilon - \varepsilon_F| > 5MeV - 10MeV$ but is much lower for states with $E \leq 5MeV$ (valence levels),

3) in mean field theory all levels are sharp (infinite mean free path), while experimentally, levels with $E > 5MeV - 10MeV$ display a damping width, i.e. a finite lifetime (cf. Fig. 2.3(d)).

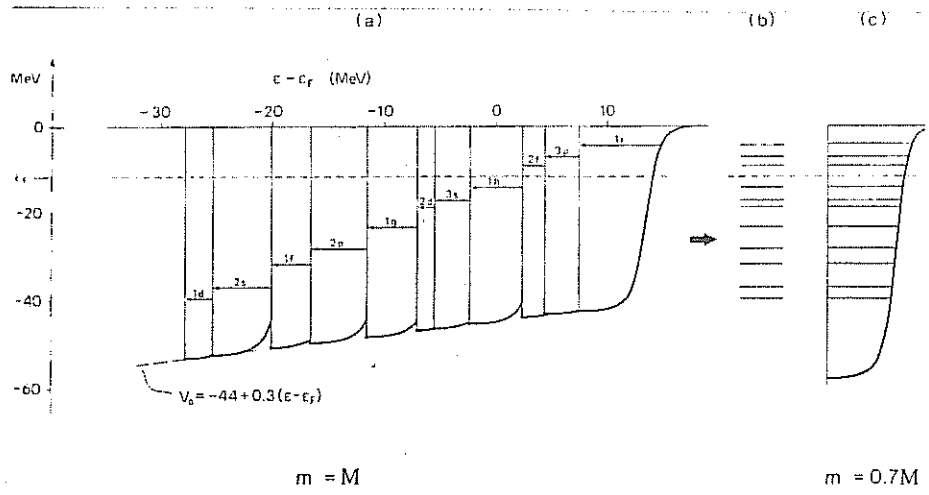


Fig. 2.8. In (a) a family of Saxon-Woods potentials with radius $R = 7.5fm$ ($A = 208$) and diffuseness $0.65fm$ is shown. The energy levels for a particle of mass $m = M$ have been calculated for all these potentials. In each of these cases one energy level is singled out. The depth $U$ of the corresponding potential has been adjusted as a function of the energy $\varepsilon_j$ of this level and follows the linear law $U = -44 + 0.3(\varepsilon_j - \varepsilon_F)$, where $\varepsilon_F = -11.5MeV$. These energy levels have been collected in (b). In (c) it is shown that essentially the same single-particle energies are obtained when using an energy-independent Saxon-Woods potential with depth $U_0 = -57MeV$ provided that the eigenstates are calculated for a particle of mass $m^* = 0.7m$ (after [7]).

The result 1) is quite natural, as $U_H(r)$ is quite similar to a Saxon-Woods potential with the parameters given in connection with Eqs.(5) and (6). The property 2) emerges because a Schrödinger equation with $m = M$ (the bare nuclear mass) and a Saxon-Woods potential of depth $U + 0.3E$ give essentially the same single-particle levels than a Schrödinger equation with $m \approx 0.7M$ and depth equal to $1.4U$ (cf. Fig. 2.8). This result explains the agreement between theory and experiment concerning the density of levels with $E > 5 - 10MeV$.

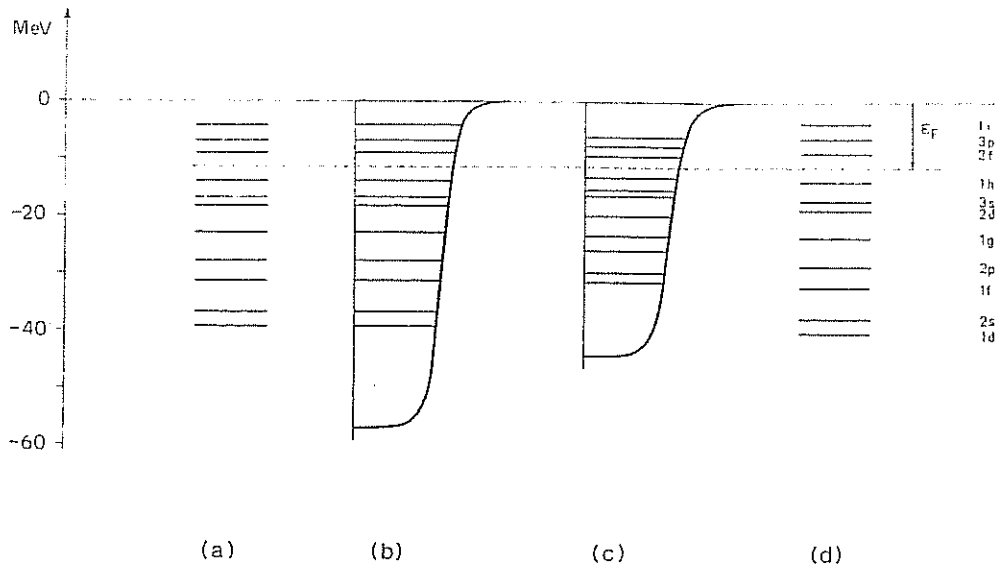


Fig. 2.9. The energy levels shown in column (a) are identical to those contained in column (a) of Fig. 2.8. Column (b) is identical to column (c) in Fig. 2.8. Column (c) displays the energy levels of a particle of mass $m$ in a Saxon-Woods potential with the same geometry and with a depth taken equal to $-44MeV$, in order to yield the same value $\varepsilon_F = -11.5MeV$ for the Fermi energy. Column (d) shows the energies obtained by multiplying by $(0.7)^{-1}$ all energy differences $\varepsilon_{nl} - \varepsilon_F$ shown in column (c).

On the other hand, the density of levels of a Schrödinger equation with $m = M$ and depth $U$ is much higher than the one with $m_k = 0.7M$, as the energy differences $\varepsilon - \varepsilon_F$ resulting from the $m_k$ Schrödinger equation are about $(\varepsilon - \varepsilon_F)/0.7$ (cf. Fig. 2.9).

The property 3) is a consequence of the fact that mean field theory defines *a surface which is rigid* *, that is, where nucleons *reflect elastically on it.* In other words, *each orbital close on itself* (cf. Fig. 2.10) and the *mean free path is infinite.* In other words, when considering the motion of an individual nucleon, the self-consistency existing between density and potential (cf. Eq.(2.5), guarantees that the motion of the $A - 1$ remaining particles adjust at each instant of time to allow a nucleon to move independently of the others, filling their pushings and pullings to change momentum at the surface.

Now, the nuclear surface can be viewed as a quantal membrane with a surface tension $\gamma \approx 1MeV/fm^2$. It is likely that it can fluctuate collectively (cf. App. Q), thus leading to an effective increase of the nuclear radius and thus to a decrease

* Of course that $U_H(r)$, being the single-particle potential associated with a many-body quantal system, displays surface fluctuations of the order of those associated with Heisenberg's relation (Eq.(1.2)).

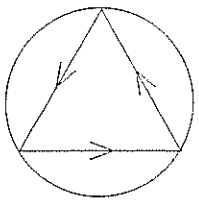

Fig. 2.10. Schematic representation of a single-particle orbital in mean field.

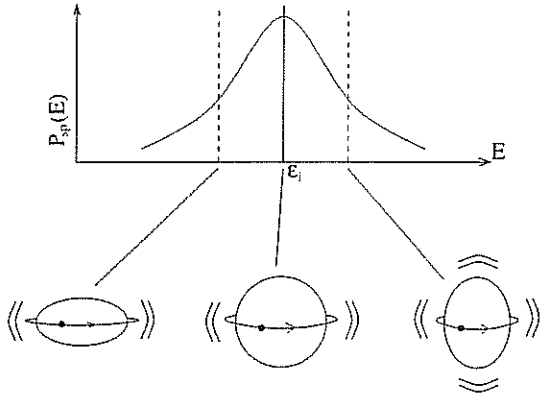


Fig. 2.11. Schematic representation of the single-particle strength function resulting from the coupling of a single-particle orbital to quadrupole fluctuations of the core.

of the kinetic energy of the nucleons. In other words, to an effective increase of the single-particle level density.

Zero-point fluctuations are also expected to lead to a damping width of single-particle levels lying away from $\varepsilon_F (> 5MeV)$. In fact, assuming an orbital concentrated along the equator, the state will feel a wider and a narrower nucleus, as a function of time, thus giving rise to a distribution of the single-particle strength (cf. Fig. 2.11).

## 2.4 Diagonalization of the complete Hamiltonian

A possible way to obtain the "exact" wavefunction of the system is to diagonalize the residual interaction $(v - U)$ in a complete basis of determinants $\Phi_n^0(\vec{r_1} \ldots \vec{r_A})$ built out of single-particle wavefunctions $\varphi_\nu(\vec{r})$, solutions of the mean field Hamiltonian $H_{MF} = T + U$ (cf. Fig. 2.12). In other words, one first calculates the absolute and the local minima and associated wavefunctions of the *constrained* mean field Hamiltonian. In this basis one calculates the matrix elements of $(v - U)$, i.e.

$$\int d^3\{r_i\}\Phi^0_n(\{\vec{r}_i\})(v-U)\Phi^0_{n'}(\{\vec{r}_i\}) = \langle \nu_1\nu_2|(v-U)|\nu_{1'}\nu_{2'}\rangle O^{A-2} \qquad (2.20)$$

where $O = \int d^3r(\varphi_\nu(\vec{r}))^*_n(\varphi_{\nu'}(\vec{r}))_{n'}$ is the overlap between two single-particle wavefunctions associated with the local minima $n$ and $n'$. Diagonalizing the resulting matrix one obtains

$$\Phi = \sum_n a^0_n \Phi^0_n, \qquad (2.21)$$

which is the "exact" solution of the problem.

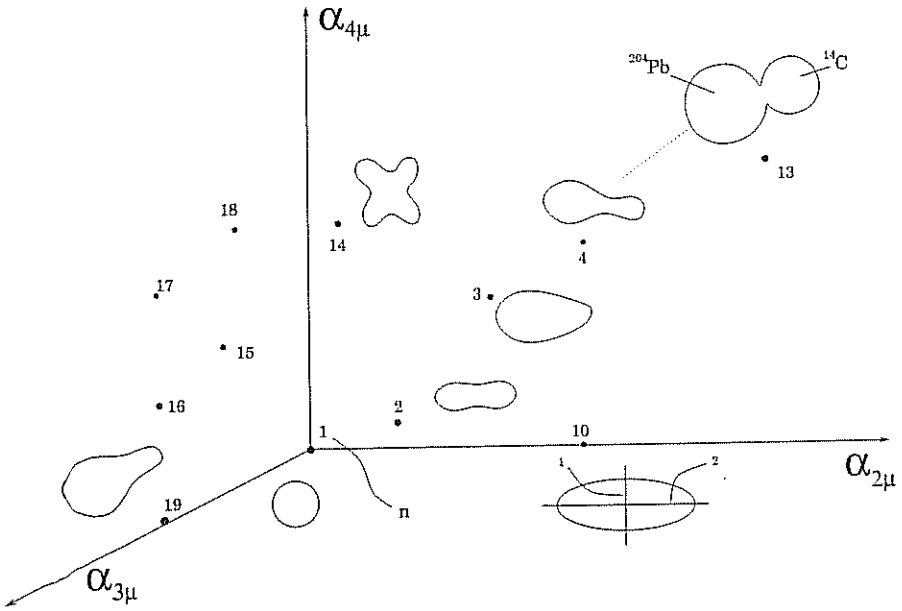


Fig. 2.12. .

In fact, to obtain such a solution, one should, in principle, include also particle-hole (and eventually many particle-many hole) states of the different local and of the absolute minimum. In any case, the function $\Phi$ given above, provides an accurate description of the exact ground state of the system.

# 3
# Collective vibration

In the nucleon-nucleus scattering experiments discussed in connection with Fig. 2.2 and used to determine the (empirical) single-particle potential $U(r)$, one has looked only at one *reaction channel*, namely the *elastic channel*, where no energy nor angular momentum is transferred between the projectile and the target, but only linear momentum. Of course, there are, in general, other channels which are open at any given bombarding energy, and which act on the elastic (entrance) channel to drain intensity from it (*absorption, imaginary part of the optical potential*), as is schematically shown in Fig. 3.1 (cf. also Eq.(4.20) and App. I).

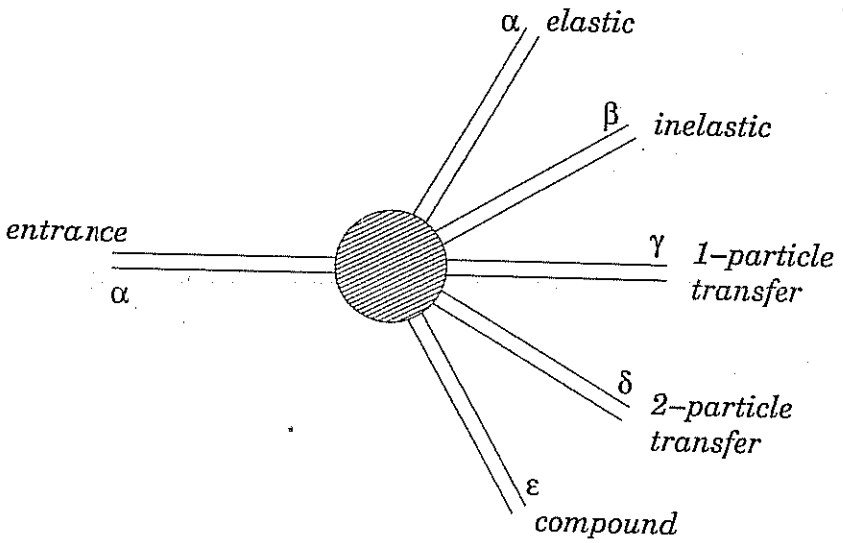


Fig. 3.1. Schematic representation of the reaction channels opened up in a nucleon-nucleus reaction.

Let us concentrate on the inelastic channel. Reactions of the type $A(p, p')A^*$ where *not only linear momentum (elastic scattering), but also energy and angular momentum are exchanged (inelastic scattering)* between a proton $p$ and a nucleus $A$ which is left in an excited state $A^*$, have shown that the nuclear surface can vibrate as a whole in well defined (normal) modes. In particular, quadrupole vibrations, of which states of up to *three phonon* have been observed (cf. Fig. 3.2) [23].

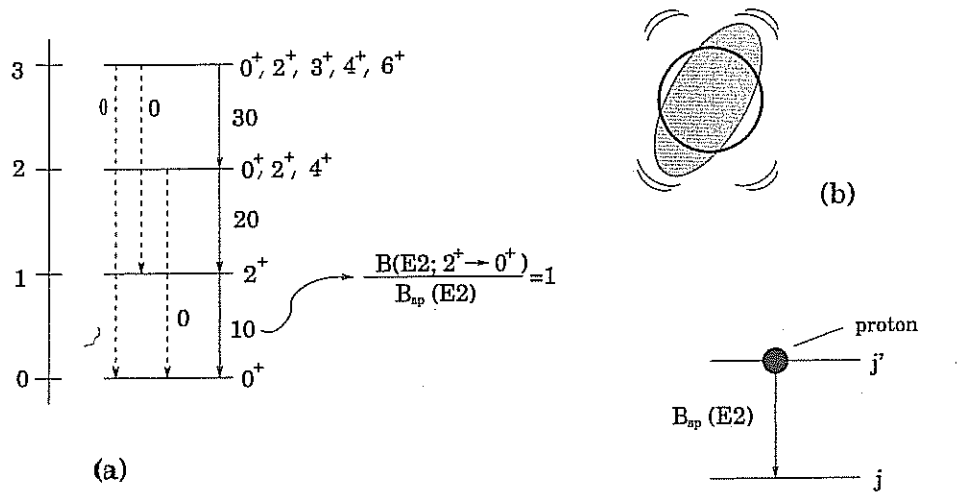


Fig. 3.2. Schematic representation of harmonic quadrupole vibrations containing up to three phonons. The transition probabilities, e.g. $B(E2; 2 \rightarrow 0) = 10$ is measured in single-particle units implying that it is 10 times stronger than a transition induced by the jump of a single proton from an excited state $j'$ to a state $j$ of lower energy.

The experimental data can be parametrized at profit making use of the (empirical) Hamiltonian

$$H_{coll} = \sum_{LM} \left( \frac{\pi_{LM}^2}{2D_L} + \frac{|\alpha_{LM}|^2}{2C_L} \right), \tag{3.1}$$

where $D_L$ and $C_L$ are the inertia and the restoring forces of the mode with multipolarity $L$. Note that the static quadrupole deformation of the mean field (Eq.(2.8) and Fig. 2.5) can be viewed as a quadrupole vibration with a restoring force $C_L$ which becomes zero.

The parameters $C_L$ and $D_L$ (which can also be calculated making use of a part of $(v - U)$) (cf. Ch. 5), can be determined from the experimental data, that is, from the energy $\hbar\omega_L$ and the transition probability $B(EL; 0 \to L)$ of the modes,

$$\hbar\omega_L = \hbar \sqrt{\frac{C_l}{D_L}}, \tag{3.2}$$

$$B(EL; 0 \to L) \sim |\langle n_L = 1 | \alpha_{LM} | 0 \rangle|^2 = \frac{\hbar\omega_L}{2C_L} \sim \beta_L^2, \tag{3.3}$$

in keeping with the fact that (cf. App. C)

$$\alpha_{LM} = \sqrt{\frac{\hbar\omega_L}{2C_L}} \left( \Gamma_{LM}^\dagger + \Gamma_{LM} \right). \tag{3.4}$$

where $|LM\rangle = |n_L = 1\rangle = \Gamma_{LM}^\dagger |0\rangle$ is the one phonon state, $\Gamma_{LM}^\dagger$ and $\Gamma_{LM}$ being the creation and annihilation boson operators fulfilling the commutation relation

$$\left[ \Gamma_{LM}, \Gamma_{LM}^\dagger \right] = 1. \tag{3.5}$$

In other words, $\alpha_{LM}$ is the coordinate of the harmonic oscillator (Dirac representation).

The Hamiltonian $H_{coll}$ (Eq.(3.1)) can then be written as

$$H_{coll} = \sum_{LM} \left( \Gamma_{LM}^\dagger \Gamma_{LM} + \frac{1}{2} \right) \hbar\omega_L \tag{3.6}$$

Consequently, with each degree of freedom there is associated a *zero point energy* $\frac{1}{2}\hbar\omega_L$ and thus a *zero point fluctuation* (cf. Fig.3.2(b)) leading to fluctuations of the nuclear radius (conserving volume so as to keep the density unchanged) which can be parametrized as (cf. also Eq.(2.8)),

$$R = R_0 \left( 1 + \sum_{LM} \alpha_{LM} Y_{LM}^*(\hat{r}) \right), \tag{3.7}$$

in keeping with the fact that the spherical harmonics provide a complete basis of eigenfunctions of the angular momentum.

# 4

# Beyond mean field: particle-vibration coupling

2.8

Inserting the expression given in Eq.(3.7) in the expression of the empirical potential given in Eq.(2.2) and expanding to lowest order in $\alpha_{LM}$ (note that $\beta_L^2 \ll \beta_L$, cf. Eq.(3.3)) one obtains

$$H = H_M + H_{coupl} + H_{coll}, \tag{4.1}$$

where

$$H_{coupl} = -\kappa \hat{\alpha} \hat{F}, \tag{4.2}$$

with

$$\hat{F} = \sum_{\nu_1 \nu_2} \langle \nu_1 | F | \nu_2 \rangle a^\dagger_{\nu_1} a_{\nu_2}, \tag{4.3}$$

and

$$F = -\frac{1}{\kappa} R_0 \frac{\partial U(r)}{\partial r} Y^*_{LM}(\hat{r}). \tag{4.4}$$

The Hamiltonian $H_{coupl}$ thus couples the motion of a single-nucleons with the collective vibrations of the surface, with a matrix element (cf. Fig.4.1)

$$\langle n_\alpha = 1, \nu' | H_{coupl} | \nu \rangle = \Lambda_\alpha \langle \nu' | F | \nu \rangle = \langle n_\alpha = 1, \nu\nu' | H_{coupl} | 0 \rangle, \tag{4.5}$$

where

$$\Lambda_\alpha = -\kappa \sqrt{\frac{\hbar\omega_\alpha}{2C_\alpha}} \sim -\frac{\kappa\beta_\alpha}{\sqrt{2L_\alpha + 1}}, \tag{4.6}$$

is the particle-vibration coupling strength. Because $\beta_L^2 \ll \beta_L$, one can usually treat the particle-vibration coupling in the weak coupling situation. Consequently $H_{coul}$, can be treated in perturbation theory. To second order one finds (cf. App. F)

$$\begin{aligned}(-\frac{\hbar^2}{2m}\nabla_r^2 &+ U_H(r))\varphi_\gamma(r) + \int \mathrm{d}^3r' U_x(\vec{r},\vec{r'})\varphi_j(\vec{r'}) \\ &+ (\Delta E + iW_j)\varphi_j(\vec{r}) \\ &\approx \left(-\frac{\hbar^2}{2m_k}\nabla_r^2 + U_H^{"}(r) + \Delta E_j + iW_j\right)\varphi_j(\vec{r}) \qquad (4.7) \\ &= \varepsilon_j\varphi_j(\vec{r}), \qquad \left(U_H^{"} = \frac{m}{m_k}U\right) \qquad (4.8)\end{aligned}$$

where (cf. Fig.4.2)

$$\Delta E_j^{(\omega)} = \mathrm{Re}\sum_j(\omega) = \lim_{\Delta\to 0}\sum_{\alpha'}\frac{V_{\nu,\alpha'}^2(\omega - E_{\alpha'})}{(\omega - E_{\alpha'})^2 + (\frac{\Delta}{2})^2} \qquad (4.9)$$

and

$$W_j^{(\omega)} = \mathrm{Im}\sum_j(\omega) = \lim_{\Delta\to 0}\sum_{\alpha'}\frac{V_{\nu,\alpha'}^2}{(\omega - E_{\alpha'})^2 + (\frac{\Delta}{2})^2} \qquad (4.10)$$

are the real and imaginary contributions to the self-energy calculated in second order perturbation theory *.

* Given a Hamiltonian $H_{coupl}$, the contribution to the energy in second order perturbation theory is

$$\Sigma_\nu(\omega) = \sum_{\alpha'}\frac{V_{\nu,\alpha'}^2}{\omega - E_{\alpha'}}, \qquad (4.11)$$

where $|\alpha'\rangle \equiv |n_a = 1, \nu'\rangle$ are the intermediate states which can couple to the initial single-particle state $\nu$. Note that the expression above is not well defined, in that the energy denominator may vanish. As a rule, textbooks in quantum mechanics deal with such a situation by stating that accidental degeneracies are to be eliminated by diagonalization. Now, this is not a real solution of the problem, because it does not contemplate the case where there are many intermediate state with $E_{\alpha'} \approx \omega$, in other words, where the particle can decay into a more complicated state, starting in the single-particle level $\nu$ of energy $\omega$, without changing its energy (real process). This is a typical dissipative (diffusion) process, and has to be solved by direct diagonalization (cf. Fig.4.5). Another way around, is to extend the function $\sum_\nu(\omega)$ into the complex plane ($E_{\alpha'} \to E_{\alpha'} + \frac{i\Delta}{2}$) thus *regularizing the divergence*, determining the finite contributions and then taking the limit for $\Delta \to 0$ (Eqs.(4.9) and (4.10)). The resulting complex potential (*optical potential* from the *complex dielectric function* of optics), parametrizes in simple terms the shift of the centroid of the single-particle state and its finite lifetime.

Furthermore,

$$E_{\alpha'} = \varepsilon_{\nu'} + \hbar\omega_{\alpha},$$

and

$$V_{\nu,\alpha'} = \langle n_{\alpha} = 1, \nu' | H_{coupl} | \nu \rangle.$$

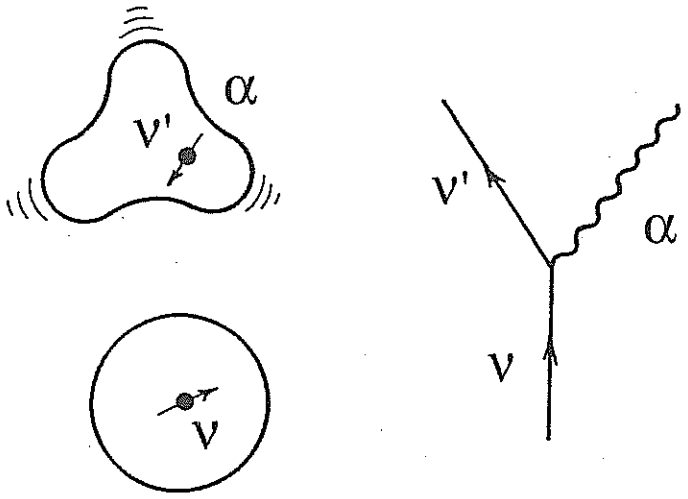


Fig. 4.1. Schematic representation of the process by which a nucleon excites the vibrations of the surface.

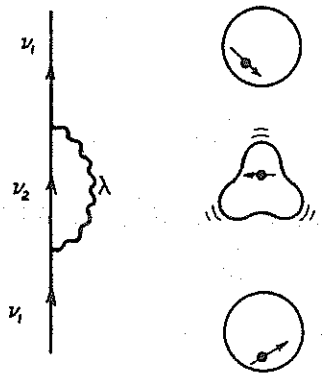


Fig. 4.2. Self-energy graph for a single-particle

For most purposes $\Delta E$ can be treated in terms of an effective mass (cf. App. C, H and Z)

$$m_\omega = m(1+\lambda), \tag{4.12}$$

where

$$\lambda = -\frac{\partial \Delta E}{\partial \omega}, \tag{4.13}$$

is the *mass enhancement factor*, while

$$Z_\omega = m/m_\omega,$$

is the spectroscopic factor (discontinuity of the Fermi energy).

Consequently, Eq.(4.8) can be rewritten as

$$\left(-\frac{\hbar^2}{2m^*}\nabla_r^2 + U'_H + iW(\omega)\right)\varphi_j(\vec{r}) = \varepsilon_j\varphi_j(\vec{r}), \tag{4.14}$$

with

$$m^* = \frac{m_k m_\omega}{m}. \tag{4.15}$$

and $U'_H = (m/m^*)U$. Because $\lambda \approx 0.5$ (i.e. the dressed single-particle $m_\omega$ is heavier than the bare nucleon, as it has to carry a phonon along), $m^* \approx 1$ and $Z_\omega \approx 0.7$. Furthermore, due to the fact that $\hbar\omega_\alpha \approx 2 - 2.5MeV$, *the range* of single-particle energy $E = \varepsilon - \varepsilon_F$ over which the particle-vibration coupling process displayed in Fig.4.2 effective is $\approx \pm 2\hbar\omega_\alpha \approx 4 - 5$ around the Fermi energy (cf. Figs.4.3 and 4.4)

To be noted that $\Delta E_j$ (Eq.(4.9)) indicates the shift in energy of the energy centroid of the "dressed" single-particle state due to the coupling to the intermediate (more complex states) $\alpha' \equiv (\nu', \alpha)$, while $\Gamma = 2W$ measures the energy range over which the single-particle state spreads due to the coupling (cf. Fig.4.5). While all states contribute to $\Delta E$ ("off the eneregy shell process", i.e. processes which do not conserve the energy), essentially only "on the energy processes", that is processes which conserve the energy, contribute to $\Gamma$. In fact

$$\lim_{\Delta\to 0} \frac{1}{(\omega - E_{\alpha'})^2 + \left(\frac{\Delta}{2}\right)^2} = 2\pi\delta(\omega - E_{\alpha'}),$$

and

$$\Gamma(\omega) \approx 2\pi\bar{V}^2 n(\omega), \tag{4.16}$$

where $\bar{V}^2$ is the average value of $V^2_{\nu,\alpha'}$, while

$$n(\omega) = \sum_{\alpha'} \delta(\omega - E_{\alpha'}), \tag{4.17}$$

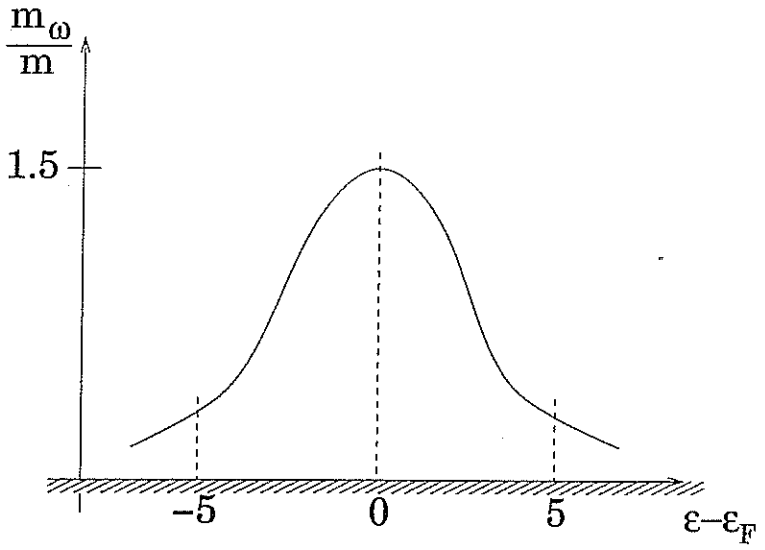


Fig. 4.3. Schematic representation of the $\omega$-mass as a function of the single-particle energy.

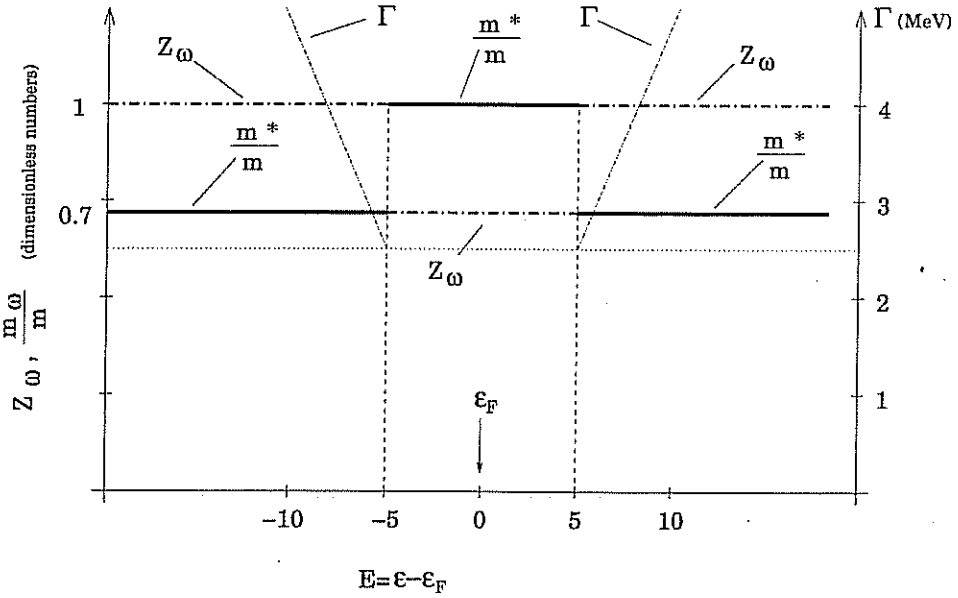


Fig. 4.4. Schematic representation of the behaviour of $m_\omega/m$, $Z_\omega = (m_\omega/m)^{-1}$ and $\Gamma$ as a function of $E = \varepsilon - \varepsilon_F$.

is the density of energy-conserving states $\alpha'$. Eq.(4.16) is known as *the Golden rule*.

On the other hand, assuming the distribution of single-particle levels is symmetric with respect to the Fermi energy

$$\Delta E(\omega) = \lim_{\Delta \to 0} \sum_{\alpha'} \frac{V^2_{\nu_1 \alpha'}(\omega - E_{\alpha'})}{(\omega - E_{\alpha'})^2 + \left(\frac{\Delta}{2}\right)^2} = 0$$

as there are equally many states pushing the state down than up (cf. Fig.4.5 and App. G).

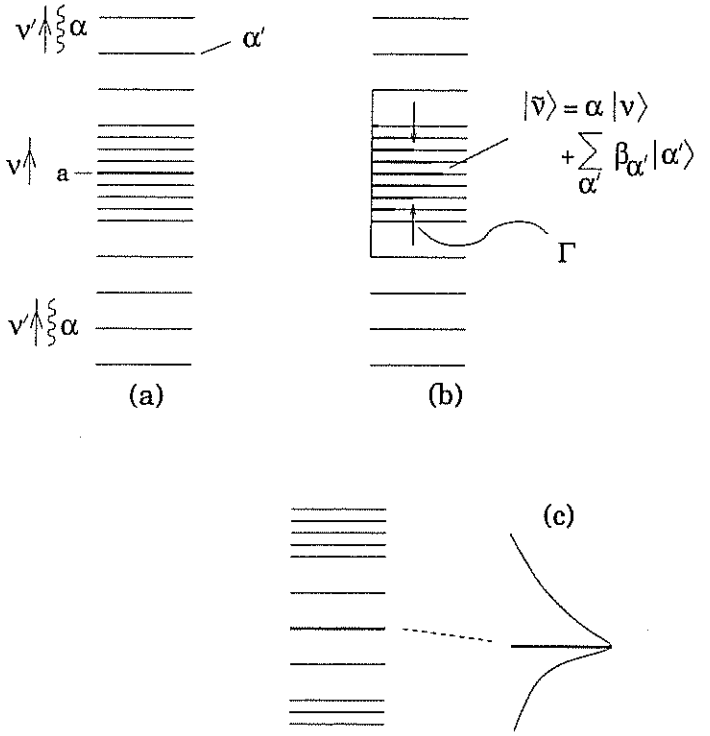


Fig. 4.5. Schematic representation of the diagonalization of $H_{coupl}$ in a basis consisting of the single-particle states $|\nu\rangle$ and the $|\alpha'\rangle = |\nu'_\alpha\rangle$ states. In (c) we show a situation where there are more states $|\alpha'\rangle$ above $|a\rangle$ than below.

Quantum mechanically there cannot be imaginary potentials, and the breaking of a stationary state into many, more complicate stationary states (Fig. 4.5(b)) is the only correct description to describe the coupling of a nucleon moving in a single-particle state with more complicate configurations †. However, such a description is quite involved. On the other hand, to account for the change of

† To be noted that if we spread the strength of a stationary quantal state over an energy range $\Gamma$, and set all components in phase at $t = 0$, they will essentially be out of phase at $t = \tau = \hbar/\Gamma$. In other words, each component will behave independent of each other and the state, created at $t = 0$ with probability 1 essentially ceases to exist at $t = \tau$.

the centroid energy and of its spreading width in terms of an *optical potential* $\Delta E + iW$ is very economic and convenient. In any case $\Gamma$ measures the range of energy over which the "pure" single-particle state $|a\rangle$ spreads due to the coupling to the more complicated states $|\alpha'\rangle$. In other words, a stationary state

$$\varphi_\nu(\vec{r}t) = e^{\frac{i\omega t}{\hbar}}\varphi_\nu(\vec{r}), \tag{4.18}$$

has a probability density

$$\int \mathrm{d}^3 r|\varphi_\nu(\vec{r}t)|^2 = \int \mathrm{d}^3 r|\varphi_\nu(\vec{r})| = 1, \tag{4.19}$$

which does not depend on time. In other words, if at $t = 0$, the probability that the particle is in a state $\nu$ is 1, it will have this probability also at $t = \infty$, implying an infinite lifetime. If however (cf. footnote 2),

$$\omega \quad = \varepsilon_\nu^{(0)} + \Delta E_\nu(\omega) + i\tfrac{\Gamma}{2}\nu(\omega), \quad = \varepsilon_\nu + i\frac{\Gamma_\nu}{2}(\omega) \qquad , (\varepsilon_\nu = \varepsilon_\nu^{(0)} + \Delta E_\nu)$$

then

$$\varphi_\nu(\vec{r}t) = e^{i\frac{\varepsilon_\nu t}{\hbar}}e^{-\frac{\Gamma_\nu t}{2\hbar}},$$

and

$$\int \mathrm{d}^3 r|\varphi_\nu(\vec{r}t)|^2 = e^{-\frac{\Gamma_\nu t}{\hbar}}, \tag{4.20}$$

implying a lifetime of the single-particle state

$$\tau = \Gamma/\hbar. \tag{4.21}$$

One may ask, how it is possible that the coupling to complicate (but still simple) states like $|\alpha'\rangle = |n_\alpha = 1, \nu'\rangle$ can explain the full damping of a single-particle state $8 - 10MeV$ from the Fermi energy $\varepsilon_F$, where the density of levels of all types is very large. This is because the Hamiltonian given in Eq. (4.1) contains all the basic physics to describe the single-particle motion. Any coupling to more complicated states will go through a hierarchy of couplings. In particular, all couplings, even the most complicate, should go through the coupling to states of type $|\nu', \alpha'\rangle$. In other words, $|\alpha'\rangle$ is a doorway state (cf. Fig.4.6).

In the nuclear case, the *doorway coupling provides the basic breaking* of the single-particle motion, while higher-order couplings only *fill in valleys* (cf. Fig.4.7). In other words, the quantity $\Gamma$ (Eq.(4.21)), gives the range over which the single-particle state is spread due to all the couplings (cf. also Fig. 2.11).

In the case of the $^1S_{1/2}$ orbital of $^{40}Ca$ ($\varepsilon - \varepsilon_F = -8$ MeV), simple estimates lead to $\bar{V}^2 \approx 0.3MeV$ for the coupling to an $L = 2$ phonon, and $n \approx 2MeV^{-1}$ (cf. App. F and P). Consequently

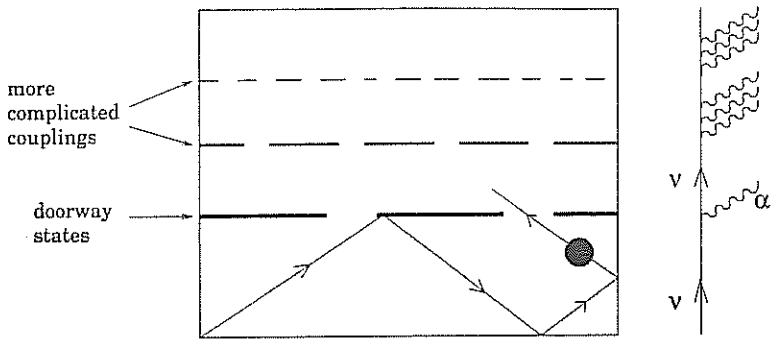


Fig. 4.6. Schematic representation of the different levels of couplings leading to the damping of a single-particle state. It is essentially the first doorway coupling which controls the probability the ball (black dot) reflecting elastically on the walls of the box has to remain in the first compartment.

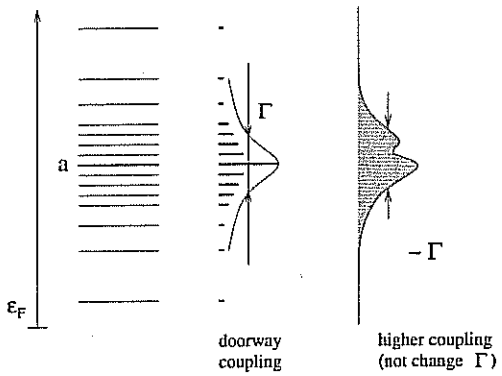


Fig. 4.7. .

$$\Gamma \approx 4MeV, \tag{4.22}$$

in overall agreement with the experimental findings (cf. Fig. 4.8).

The result given in Eq.(4.22) is a particular example of the general (empirical) result (cf. Fig. 4.4)

$$\Gamma_{sp}(E) = \begin{cases} 0.5E & E > 5 \text{ MeV}, \\ 0 & E \leq 5 \text{ MeV}, \end{cases} \tag{4.23}$$

where

$$E = |\varepsilon - \varepsilon_F|. \tag{4.24}$$

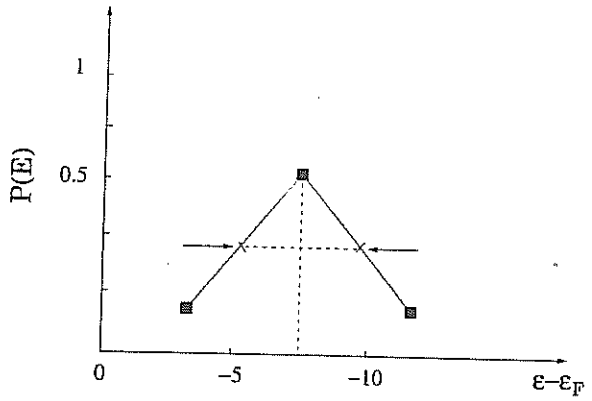


Fig. 4.8. Schematic representation of the experimental strength function (solid squares) associated to the $1s$ state of $^{40}Ca$. Also indicated is the full width at half maximum (FWHM) (after [7]).

## 4.1 Induced interaction

A nucleon at the Fermi energy which creates, by bouncing inelastically off the nuclear surface, has no other choice but to reabsorb it at a later instant of time (virtual process, Fig. 4.2). In the presence of another nucleon, the vibration excited by one nucleon may be absorbed by the second one (Fig.4.9), the exchange of a vibration leading to an (induced) interaction.

Simple estimates of this induced interaction lead to values of the matrix element for pairs of particles coupled to angular momentum $J^\pi = 0^+$ of $-1.5MeV$, when summed over all the different multipolarities $\alpha$ ($L^\Pi = 2^+, 3^-, 5^-$) (cf. App. F). The fact that one considers particles coupled to anguler momentum zero is because the associated orbitals have maximum overlap, thus profiting at best from the (pairing) interaction ‡. In the case of two particles outside closed shell one would then expect the ground state to display, due to this mechanism, a correlation energy of $1.5MeV$ larger than that predicted by the independent particle model (cf. Fig.4.10), a prediction which is confirmed by the experimental findings.

From this result one can conclude that the pairing interaction induced by the process depicted in Fig.4.9, renormalize in an important way the properties of the nuclear ground state of open shell nuclei.

‡ Note that quadrupole pairing correlations are also important, although weaker.

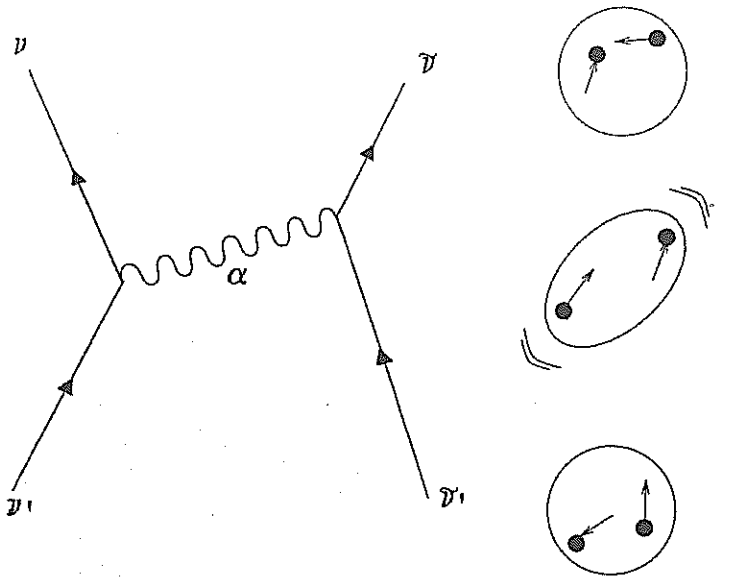


Fig. 4.9. Schematic representation of the exchange of phonons between nucleons.

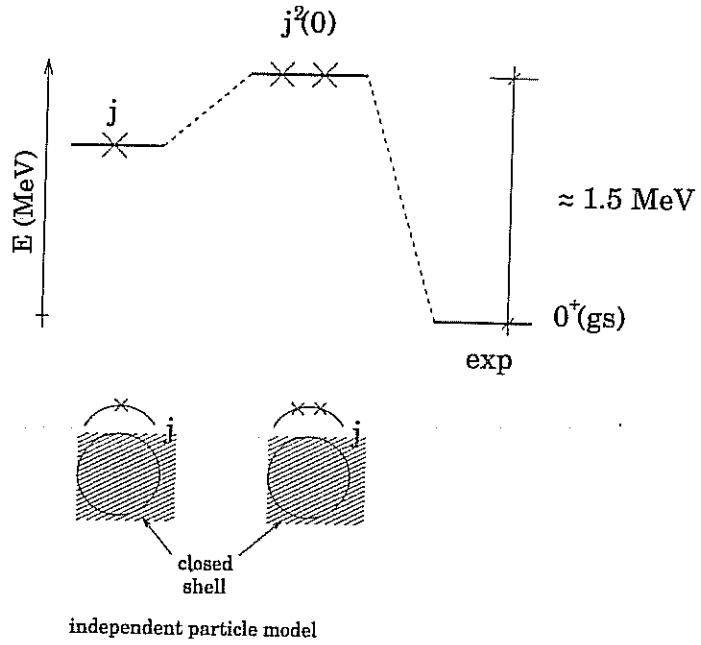


Fig. 4.10. Schematic representation of the predictions of the independent particle model for one- and two-particles outside closed shell, in comparison with the experimental findings (e.g. for the case of $^{210}Pb$, where $j = g_{9/2}$).

# 5

# Collective vibrations: microscopic description

In a self substained vibration (normal mode), the variations of the potential must be self consistent with those of the density. In other words, the relation given in Eq.(2.5) is also required to be valid for the dynamical situation, that is,

$$\delta U = \int \mathrm{d}^3 r' \delta\varrho v(|\vec{r} - \vec{r}'|). \tag{5.1}$$

In fact, one can excite the system: (a) by acting collectively on the nucleus and deforming slightly the potential $U$ (thus leading to $\delta U$), (b) promoting a particle from below to above the Fermi energy with a given probability (thus leading to $\delta\varrho$) (Fig.5.1), in keeping with the fact that a single-particle external field can change the state of motion of one particle at a time.

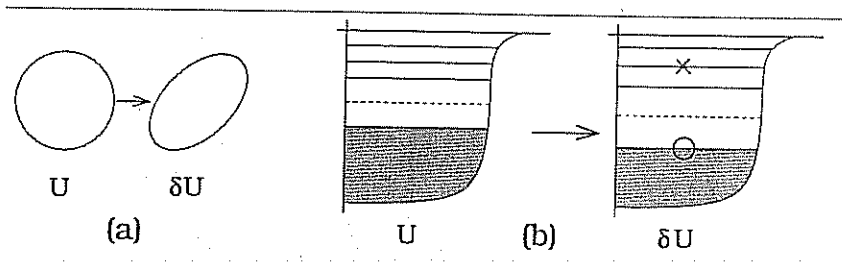


Fig. 5.1. Complementary views of the nucleus: a) as a sytem confined by an elastic surface, or b) as a many-particle determinant.

Another representation of Eq. (5.1) can be made through $\hat{\alpha}$ and $\hat{F}$, as shown in Fig.5.2 (cf. also App. E).

Making use of the relation shown in this figure, one finds

$$\frac{1}{\kappa} = \sum_{ki} \frac{2(\varepsilon_k - \varepsilon_i)\langle k|F|i\rangle^2}{(\varepsilon_n - \varepsilon_i)^2 - (\hbar\omega_\alpha)^2}. \tag{5.2}$$

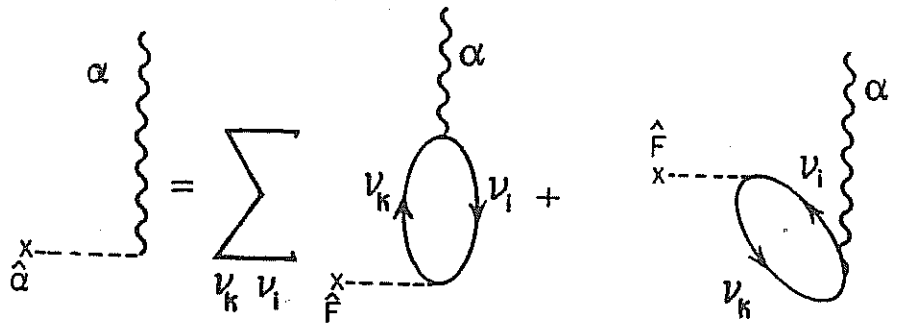


Fig. 5.2. Relation used to calculate the vibrational frequencies.

This dispersion relation determines the frequencies $\hbar\omega_\alpha$ of the vibrational modes (cf. Fig.5.3).

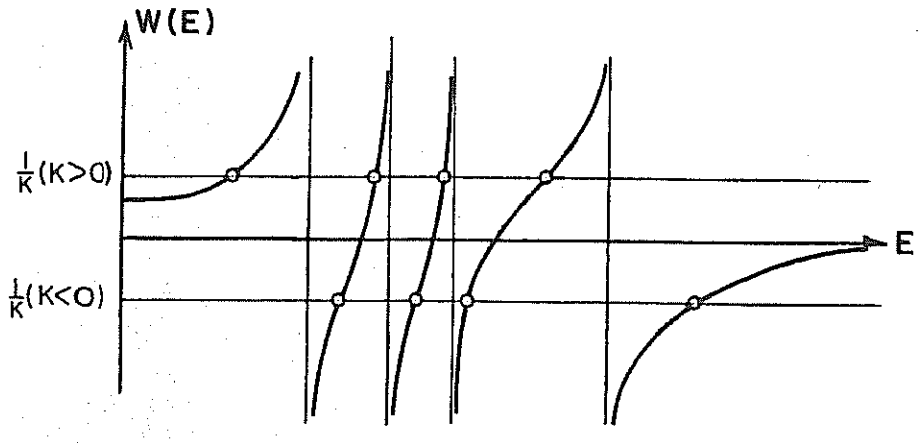


Fig. 5.3. Graphical solution of the dispersion relation given in Eq.(5.2).

Because the low-lying mode, i.e. the solution $\hbar\omega_1$ falls inside the lowest particle-hole excitation $(\varepsilon_k - \varepsilon_i)_1$, its properties will depend on the properties of the ground state, in particular the pairing correlations.

We shall thus use Eq.(5.2) only to calculate the collective high-lying modes, known as *giant resonances* [24]. The discussion of the low-lying vibrational modes is taken up in Ch. 16.

To further simplify the calculations one can make use of and oscillator potential to describe the single-particle motion (cf. Fig.5.4). In the case of the dipole vibration, $F = z$, and $(\varepsilon_k - \varepsilon_i) = \hbar\omega_0$, because $\langle k|F|i\rangle = \langle N'|F|N\rangle \sim \delta(N', N \pm 1)$, where $N$ is the principal quantum number of an harmonic oscillator shell. Con-

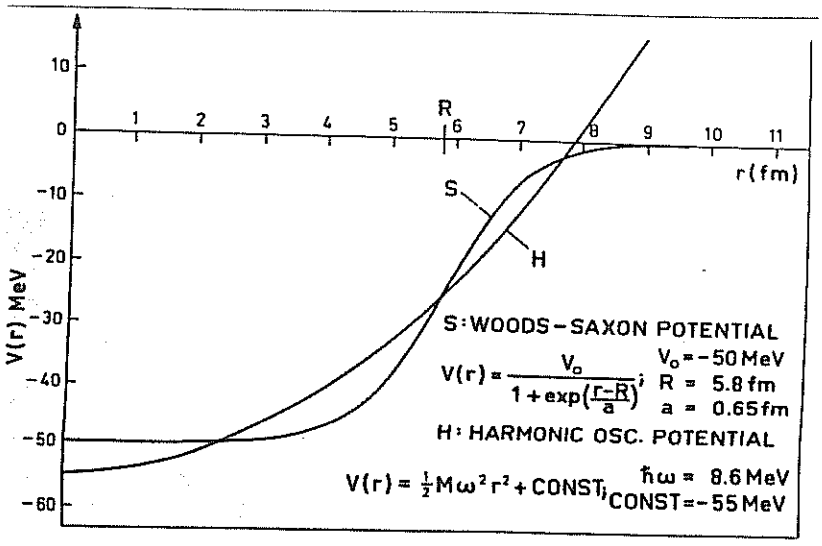


Fig. 5.4. Schematic representation of a Saxon-Woods potential describing a nucleus of mass number $A \approx 114$ and of an harmonic oscillator potential displaying the same mean square radius (after [22]).

sequently, Eq.(5.2) becomes

$$\frac{1}{2\kappa} = \frac{\sum_{ki}(\varepsilon_k - \varepsilon_i)\langle k|z|i\rangle^2}{(\hbar\omega_0)^2 - (\hbar\omega_D)^2}. \tag{5.3}$$

The sum in the numerator is the maximum energy the system can absorb in a photoabsorption process. It can be shown to be equal to (cf. App. AE)

$$\begin{aligned} S(F) &= \frac{1}{2}\langle 0|\,[[H,F],F]\,|0\rangle \\ &= \frac{\hbar^2}{2M}\int \mathrm{d}^3 r|\vec{\nabla}F|^2\rho_0(r) = \frac{\hbar^2 A}{2M}, \end{aligned} \tag{5.4}$$

(5.5)

which is known as the Thomas-Reiche-Kuhn (TRK) sum rule. It states the fact that, under an instantaneous sollicitation, the nucleus reacts as a system of $A$ uncorrelated nucleons, which acquire a finite kinetic energy $\frac{\hbar^2}{2M}|\vec{\nabla}F|$ per nucleon. The fact that this number depends only on the mass number $A$ of the nucleus, and the nucleon mass $M$, testifies to the model independence of the EWSR result.

Because the collective modes $\alpha$ are a linear combination of particle hole excitations,

$$\Gamma^{\dagger}_{\alpha} = \sum_{ki} X^{\alpha}_{ki}(a^{\dagger}_{k}a_{i}) + Y^{\alpha}_{ki}(a^{\dagger}_{k}a_{i})^{\dagger}, \tag{5.6}$$

expressing the fact that while the collective modes look very simple in the collective representation of vibrations, they appear quite a bit more complicated (although more microscopic), in the particle-hole basis (cf. also Fig.5.2). Making use of the unitary transformation given by Eq.(61), one can show that $\hat{\alpha} = \hat{F}$ (App. E). Consequently

$$H_{coupl} = -\kappa\hat{\alpha}\hat{F} = -\kappa\hat{F}\hat{F}, \tag{5.7}$$

This is a two-body force which inserted into Eq.(5.1), together with the ansatz (volume mode)

$$\delta\rho_1 \sim z\rho_0,$$

and the relation (cf. Eq.(2.3))

$$\delta U_1 = V_1\delta\left(\frac{N-Z}{A}\right) = V_1\frac{\delta\rho_1}{\rho_0},$$

allows one to calculate $\kappa_1 = -5V_1/AR^2$. This quantity, together with the TRK sum rule and Eq.(5.3), leads to

$$\begin{aligned}\hbar\omega_D &\approx \frac{80}{A^{1/3}}\text{MeV} \\ &\approx \frac{100}{R}\text{MeV},\end{aligned} \tag{5.8}$$

($R = 1.2A^{1/3}$fm), a number which is very close to the experimental value (cf. Fig. 5.5). The inverse dependence with the radius (momentum dependence) is typical of elastic vibrations.

In the case of quadrupole vibrations, one obtains

$$\hbar\omega_Q = \frac{60}{A^{1/3}}\text{MeV}, \tag{5.9}$$

which provides an overall account of the experimental findings.

In other words, the nucleus reacts elastically with a dipole mode of energy $\approx$ 16 MeV and carrying $\approx$ 100% of the TRK and with $\approx$ 12 MeV and again $\approx$ 100% of the EWSR to an external to quadrupole field.

While mean field theory predicts the states to be sharp, experimentally they display a resonant behaviour with a width of the order of 30% of the centroid energy (cf. Fig.5.6).

Similar to what was found in the case of single-particle motion, the coupling of the giant resonance to the zero point fluctuations of the ground state accounts

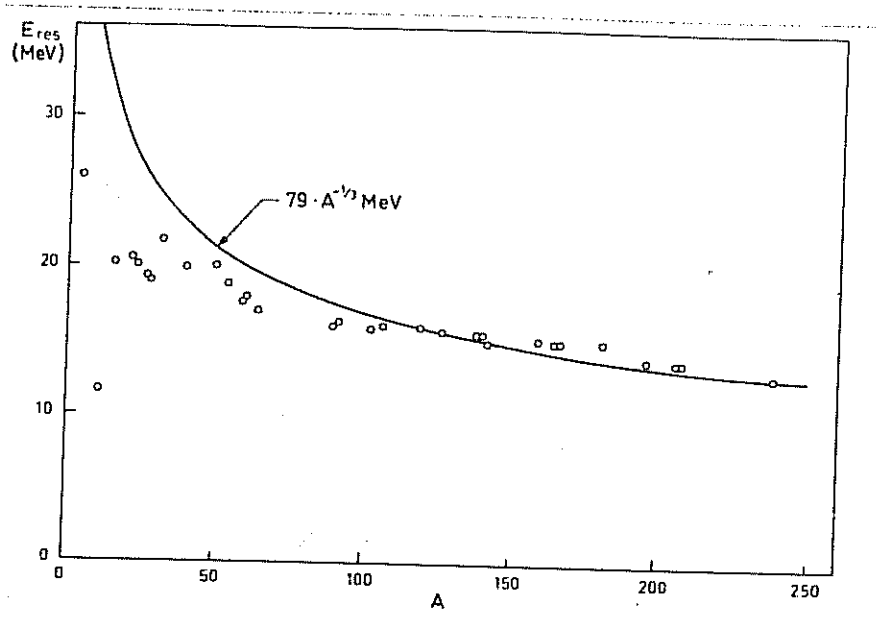


Fig. 5.5. Schematic representation of the energy centroid of the GDR (giant dipole resonance). The open circles are the experimental data (after [22], cf. also [24]).

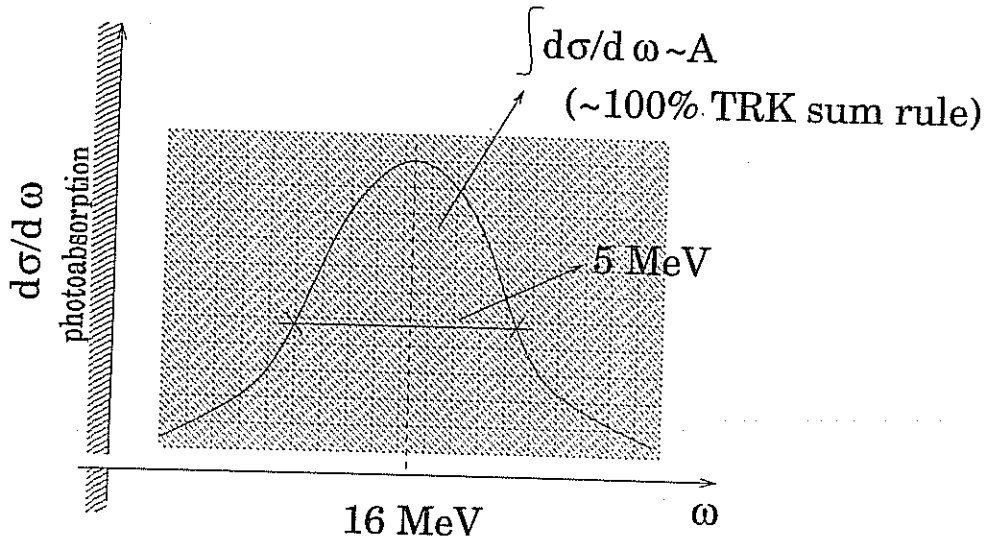


Fig. 5.6. Schematic representation of the photoabsorption cross section as a function of the photon frequency $\omega$ for a nucleus of mass number $\approx 120$.

for the spreading width. This is because elastic vibrations are inversely proportional to the nuclear radius (cf. Eq.(5.9)). In particular, in the case of the dipole

resonance, quadrupole fluctuations of the nuclear surface are particularly effective (note that a $1^-$ can, to give a gain of $1^-$, couple only to $0^+$ and to $2^+$). This effect is schematically shown in Fig.5.7 (cf. also Fig.2.11).

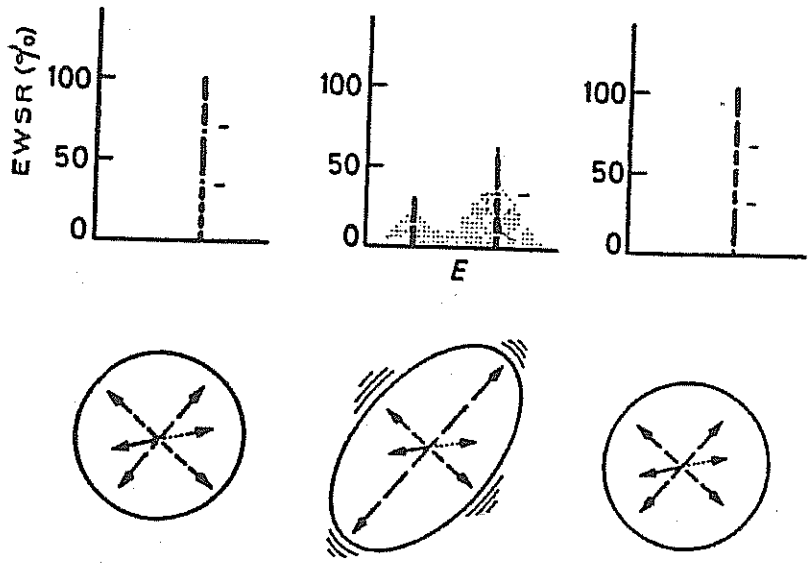


Fig. 5.7.

The damping width of giant resonances can be calculated microscopically. In fact, because giant resonances are linear combinations of particle-hole excitations, the width of a GR can be estimated to be the sum of the width of the particle and of the hole, that is

$$\Gamma_{GR}(\hbar\omega_{GR}) = \Gamma_p\left(\frac{\hbar\omega_{GR}}{2}\right) + \Gamma_h\left(\frac{\hbar\omega_{GR}}{2}\right) \tag{5.10}$$

where we have assumed that half of the energy of the giant resonance is taken up by the particle and half by the hole (note that we are considering an energy conserving process). Making use of the relation given in Eq. (4.23) valid for both particles and holes one obtains

$$\Gamma_{GR}(E_{GR}) = 0.5E_{GR}. \tag{5.11}$$

For the dipole resonance this relation gives

$$\Gamma_D \approx \frac{40}{A^{1/3}}\text{MeV} \approx 8\text{MeV}, \tag{5.12}$$

a number which is appoximately a factor of 2 larger than that experimentally observed.

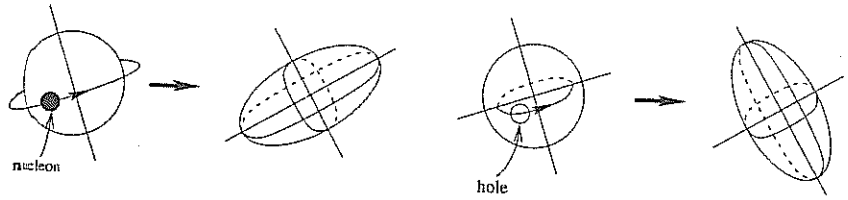


Fig. 5.8. .

The reason for this result lies in the fact that in the expression given in Eq.(5.9) we do not consider the possible exchange of vibrations between a particle and a hole, but consider only processes where a particle, or a hole, both excite and reabsorb the vibration.

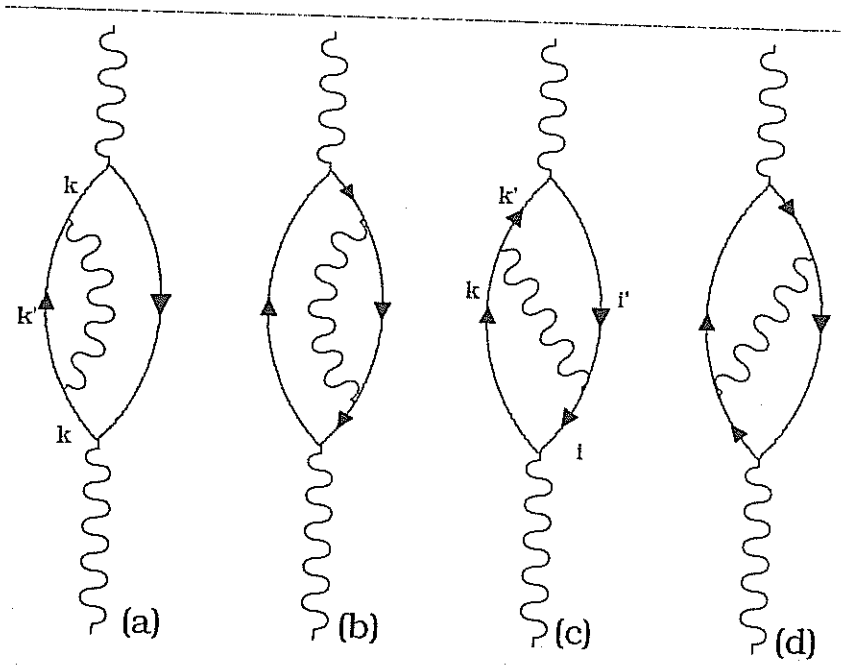


Fig. 5.9. Lowest order processes contributing to the damping of giant resonances. Graphs (a) and (b) are directly related to the damping of single-particle and single-hole motion. Processes (c) and (d) are so called vertex renormalization processes.

In a normal mode like a giant dipole vibration, particles and holes are correlated so as to produce a collective vibration. While the process shown in Figs. 5.9 (a) and (b) make the particle (hole) heavier thus decreasing the correlation existing among them and as a consequence leading to a finite lifetime, processes

5.9 (c) and (d) try to glue the particle to the hole increasing the correlation between them (cf. also Fig. 4.9). In other words, the amplitudes associated with the processes (c) and (d) have sign opposite to those of (a) and (b), and reduce the estimate given in Eq.(5.12) to the correct observed value (cf. App. Ö). This is because

$$\langle hole|H_{coupl}|hole\rangle = -\langle particle|H_{coupl}|particle\rangle$$

for low-lying surface vibrations ($\alpha = 2^+, 3^-, 5^-$), a result that is intimately connected to the fact that e.g. the quadrupole deformations induced by a nulceon moving around close shell has opposite sign than that induced by the lack of a nucleon (hole) (cf. Fig. 5.8).

# 6

# Pairing: experimental facts

The nuclear binding energy is found to exhibit a systematic variation depending on the evenness or oddness of $Z$ and $N$,

$$\delta\mathcal{B} = \begin{cases} \Delta & Z \text{ even}, N \text{ even}, \\ 0 & A \text{ odd}, \\ -\Delta & Z \text{ odd}, N \text{ odd}, \end{cases} \tag{6.1}$$

where

$$\Delta = -\frac{1}{2}\left\{\mathcal{B}(N-1,Z) + \mathcal{B}(N+1,Z) - 2\mathcal{B}(N,Z)\right\},$$

and $\mathcal{B}(N,Z)$ is the total binding energy and represents the diffrence between the observed mass $\mathcal{M}$ (or, equivalently, the total nuclear energy $\mathcal{E}$), in the ground state and the masses of the separated nucleons,

$$\mathcal{M}(N,Z) = \frac{1}{c^2}\mathcal{E}(N,Z) = NM_n + ZM_p - \frac{1}{c^2}\mathcal{B}(N,Z).$$

The observed pairing energies (Fig. 6.1) can be parametrized according to

$$\Delta \approx \frac{12}{\sqrt{A}}\text{MeV}. \tag{6.2}$$

The large odd-even effect observed may be described in terms of pairwise correlations of identical particle coupled to angular momentum zero, which contribute an additional binding energy $2\Delta$ per pair, for nucleons on top of the Fermi surface (cf. also Sect. 4.1). Consistent with the above findings, the lowest non-collective excitations in even-even nuclei are found at an energy of $\approx 2\Delta$.

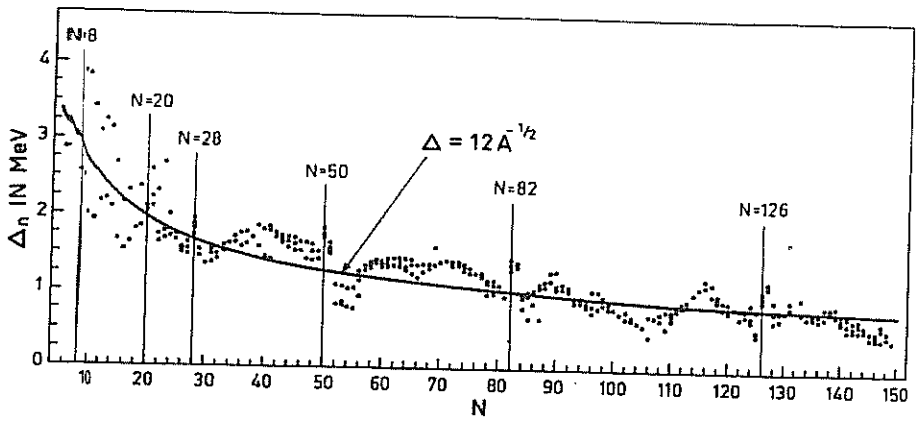


Fig. 6.1. Odd-even mass difference for neutrons (after [22]).

## 6.1 Pairing interaction

A schematic interaction producing such an effect is the pairing force with constant matrix elements (cf. Fig. 6.2 and App. D)

$$H_p = -G \sum_{\nu,\nu'>0} a^\dagger_\nu a^\dagger_{\bar{\nu}} a_{\bar{\nu}'} a_{\nu'}.$$

where the state $a^\dagger_{\bar{\nu}}|0\rangle = |\bar{\nu}\rangle$ is the time-reversal state to $a^\dagger_\nu|0\rangle = |\nu\rangle$. Making use of the fact that $a^\dagger_{\bar{\nu}} = a_{j_\nu \widetilde{m_\nu}} = (-1)^{j_\nu - m_\nu} a^\dagger_{j_\nu - m_\nu}$, and that the Clebsch-Gordon coefficient which couples two tensors of equal rank to total angular momentum zero is proportional to $(-1)^{j_\nu - m_\nu}$, i.e. $\langle j_\nu m_\nu j - m_\nu | 00\rangle = (-1)^{j_\nu - m_\nu}/\sqrt{2j_\nu + 1}$, it is easy to show that $\sum_{\nu>0} a^\dagger_\nu a^\dagger_{\bar{\nu}} \sim (a^\dagger_\nu a_\nu)_{00}$ (cf. Apps. W, X and Y). In other words, the pairing interaction scatters, across the Fermi energy, pairs of particles, coupled to angular momentum zero.

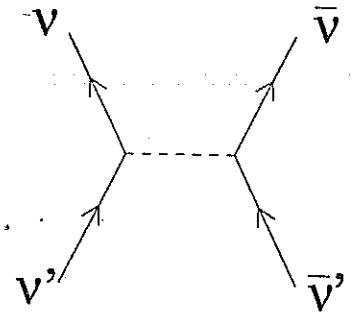


Fig. 6.2. Schematic representation of the pairing interaction.

To understand the consequences of particles moving in single-particle orbits

interacting throgh a pairing force, i.e. particles controlled by the Hamiltonian

$$H = H_{sp} + H_p, \tag{6.3}$$

where

$$H_{sp} = \sum_{\nu>0} (\varepsilon_\nu - \lambda)(a^\dagger_\nu a_\nu + a^\dagger_{\bar{\nu}} a_{\bar{\nu}}), \tag{6.4}$$

and where the single-particle energies are measured with respect to the Fermi energy $\varepsilon_\lambda$ which we shall call $\lambda$ following the literature, not to be confused with the mass enhancement factor defined in Eq. (44).

We shall diagonalize the Hamiltonian given in Eq.(6.3), making use of the ansatz that the pairing interaction does not change the single-particle energies $\varepsilon_\nu$, nor the associated wavefunction $\varphi_\nu(r)$ obtained by solving the (renormalized) Hartree-Fock eqs.(4.14) and (4.15). This is because the average pairing matrix element (cf. Sect. 7.1) $\langle (j)^2_0 | H_p | (j')^2_0 \rangle = -\frac{G}{2}\frac{(2j+1)}{2} \approx -0.4$MeV (for medium heavy mass nuclei, i.e. nuclei with $A \approx 120$) is small compared with typical matrix elements of the average single-particle potential (of depth $V_0 = -50$MeV), as well as with the separation energy between major shells ($\hbar\omega_0 \approx 41/A^{1/3}$MeV $\approx 8$MeV).

On the other hand, $G$ is of the order of the separation of single-particle levels of open shell nuclei lying close to the Fermi energy ($1 - 2$MeV for spherical nuclei 0.5MeV for deformed nuclei). Consequently, one expects the main effect of $H_p$ at the level of mean field is to change the occupancy of single-particle states around the Fermi surface.

## 6.2 Simple estimate of the matrix elements

Let us assume $\nu = (j, m)$. Thus

$$\begin{aligned}
\sum_{\nu>0} a^\dagger_\nu a^\dagger_{\bar{\nu}} &= \sum_{jm>0} a^\dagger_{jm} a^\dagger_{\bar{jm}}, \\
&= \frac{1}{2}\sum_{jm} a^\dagger_{jm} a^\dagger_{\bar{jm}} = \frac{1}{2}\sum_{jm} (-1)^{j-m} a^\dagger_{jm} a^\dagger_{j-m}, \\
&= \frac{1}{2}\sqrt{2j_\nu + 1}\sum_{jm} \langle jmj - m|00\rangle a^\dagger_{jm} a^\dagger_{j-m}, \\
&= \frac{1}{2}\sqrt{2j_\nu + 1}\sum_{j} (a^\dagger_j a^\dagger_j)_{00}.
\end{aligned} \tag{6.5}$$

Consequently

$$H_p = -\frac{G}{2}\sum_{jj'}\sqrt{\Omega_j\Omega_{j'}}(a_j^\dagger a_j^\dagger)_0(a'_j a'_j)_0,$$

where

$$\Omega_j = \frac{2j+1}{2}. \tag{6.6}$$

Thus

$$\langle (j,j);0|H_p|(j',j')0\rangle = -\frac{G}{2}\sqrt{\Omega_j\Omega_{j'}} \approx -\frac{G}{2}\frac{2j+1}{2}$$

Making use of the average value of the angular momentum for a nucleus of radius $R$ (cf. App. P),

$$\begin{aligned}\bar{j} &\approx Rk_F = 1.2A^{1/3}\text{fm}\times 1.36\text{fm}^{-1}\\ &\approx 1.6A^{1/3}\approx 8 \quad (A\approx 120),\end{aligned} \tag{6.7}$$

and

$$G \approx \frac{25}{A}\text{MeV} \approx 0.2\text{MeV}, \tag{6.8}$$

one obtains

$$\langle (j,j)0|H_p|(j',j')0\rangle \approx -\frac{0.2\text{MeV}\times 8}{4} \approx -0.4\text{MeV}. \tag{6.9}$$

# 7

# Mean field, BCS solution of pairing

Let us diagonalize the Hamiltonian introduced in Eq.(6.3) in the mean field approximation (App. O). For this purpose, we have to extract a single-particle field from the two-body interaction

$$H_p = -GP^\dagger P, \tag{7.1}$$

where

$$P^\dagger = \sum_{\nu>0} a^\dagger_\nu a^\dagger_{\bar{\nu}}. \tag{7.2}$$

In other words, we have to extract from $H_p$, a bilinear expression in the creation and annhilation operators. For this purpose we define the expectation value

$$\alpha_0 = \langle BCS|P^\dagger|BCS\rangle = \langle BCS|P|BCS\rangle, \tag{7.3}$$

where the ground state of the mean field of the Hamiltonian given in Eq.(6.3) has been denoted $|BCS\rangle$ (the Bardeen, Cooper, Schrieffer ground state of the system [25]). Although we do not know it yet, we assume it exists.

One can now write Eq.(7.1) as

$$H_p = -G\left[(P^\dagger - \alpha_0) + \alpha_0\right]\left[(P - \alpha_0) + \alpha_0\right], \tag{7.4}$$

and assume that the matrix elements of $(P^\dagger - \alpha_0)$ and of $(P - \alpha_0)$ in the state $|BCS\rangle$ are much smaller than $\alpha_0$. In other words, that the average value of the two-particle transfer operators $P^\dagger$ and $P$ are larger than the associated fluctuations. Thus, neglecting quadratic terms in these fluctuations, Eq.(7.3) gives the pairing field

$$V_p = -\Delta(P^\dagger + P), \tag{7.5}$$

where

Consequently, $(H_p)_{MF}$ is now diagonal, sum of two terms namely

$$U = 2\sum_{\nu>0}(\varepsilon_\nu - \lambda)V_\nu^2 - \frac{\Delta^2}{G}, \tag{7.18}$$

and

$$H_{11} = \sum_{\nu>0} E_\nu \alpha_\nu^\dagger \alpha_\nu. \tag{7.19}$$

The parameters $U_\nu$ and $V_\nu$ which completely define the BCS mean field solution of the pairing Hamiltonian depend on the Fermi energy $\lambda$ and the gap parameter $\Delta$. The equations determining these parameters are the number equation

$$N = \langle BCS|\hat{N}|BCS\rangle = 2\sum_{\nu>0} V_\nu^2, \tag{7.20}$$

where

$$\hat{N} = \sum_{\nu>0} a_\nu^\dagger a_\nu, \tag{7.21}$$

is the operator number of particles operator, and the gap equation

$$\Delta = G\langle BCS|P^+|BCS\rangle = G\sum_{\nu>0} U_\nu V_\nu. \tag{7.22}$$

In other words

$$\begin{aligned} N &= 2\sum_{\nu>0} V_\nu^2, && \text{(number equation)} \\ \frac{1}{G} &= \sum_{\nu>0}\frac{1}{2E_\nu}, && \text{(gap equation)} \end{aligned} \tag{7.23}$$

allow to calculate $\lambda$ and $\Delta$ from the knowledge of $\varepsilon_\nu$ and of $G$.

While the ground state energy is equal to $U$, the energy of the lowest excited state, that is, that of a two-quasiparticle state, generalization of a particle-hole excitation in the case of normal ($G = 0$) systems, is

$$H_{11}|\nu_1\nu_2\rangle = H_{11}\alpha_{\nu_1}^\dagger \alpha_{\nu_2}^\dagger |BCS\rangle = (E_{\nu_1} + E_{\nu_2})|\nu_1\nu_2\rangle. \tag{7.24}$$

Consequently, there are no excited states with energy less than $2\Delta$, the minimum value of $(E_{\nu_1} + E_{\nu_2})$.

Properly adjusting $G$ for a given value of particles $N$, one can make this excitation to coincide with twice the value given in Eq.(6.2). Also to correlate the ground state, by the amount needed to reproduce the odd-even staggering expressed by Eq.(6.2). This value is

Notes Achim Schwenk — bare vs self consistent [$\lambda = GN(0)$])
$\lambda \to \Delta$ strong and weak coupl.

## II. COOPER PAIRS

Section Pair... structure

The presence of (Cooper pairs)

The pairing interaction correlates pairs of nucleons moving in time reversal states over lengths of the order of $\xi = \hbar v_F / E_{corr}$, much larger than nuclear dimensions (cf. e.g. [3]), in keeping with the fact that the associated two–nucleon correlation energy is $E_{corr} \approx 0.5$–$2$ MeV. These extended, strongly overlapping virtual objects, known as Cooper pairs, affect most of the properties of nuclei close to their ground state, as well as of their decay. ~~A textbook~~

This is a natural consequence of the fact that Cooper pair formation and then eventual condensation (also virtual), not only introduces a new energy length (pairing gap) over which the Fermi energy becomes blurred like in the case of an effective (quantal) temperature, but furthermore it changes the statistics of the associated degrees of freedom.

An example of the central role pairing correlations have on the properties of atomic nuclei

example of ~~this last assertion~~ is provided by the exotic decay $^{223}\mathrm{Ra} \rightarrow ^{209}\mathrm{Pb} + ^{14}C$. The measured decay constant $\lambda = 4.3 \times 10^{-16}\mathrm{s}^{-1}$, implies that the wavefunction describing the ground state of the superfluid nucleus $^{223}$Ra has a component of amplitude of about $10^{-5}$ corresponding to a shape closely resembling $^{209}$Pb in contact with $^{14}$C. But this requirement can be fulfilled only if this exotic, strongly deformed system, is superfluid. In other words, if pairs of nucleons are correlated over distances of the order of 20 fm, sum of the Pb and C diameters [12].

### A. Pairing correlations

Nuclear superfluidity can be studied at profit in terms of the mean field, BCS diagonalization of the pairing Hamiltonian [13], namely,

$$H = H_{sp} + V_p, \tag{1}$$

where

$$H_{sp} = \sum_{\nu} (\epsilon_\nu - \lambda) a_\nu^+ a_\nu, \tag{2}$$

while

$$V_p = -\Delta(P^+ + P) - \frac{\Delta^2}{G}, \tag{3}$$

and

$$\Delta = G\alpha_0, \tag{4}$$

is the pairing gap ($\Delta \approx 12$ MeV$/\sqrt{A}$), $G$ ($\approx 25$ MeV$/A$ ) being the pairing coupling constant [3], and

$$P^+ = \sum_{\nu>0} P_\nu^+ = \sum_{\nu>0} a_\nu^+ a_{\bar{\nu}}^+, \tag{5}$$

$$P = \sum_{\nu>0} a_{\bar{\nu}} a_\nu, \tag{6}$$

are the pair addition and pair removal operators, $a_\nu$ and $a_\nu^+$ being single-particle creation and annihilation operators, $(\nu\bar{\nu})$ labeling pairs of time reversal states.

The BCS ground state wavefunction describing the most favorable configuration of pairs to profit from the pairing interaction, can be written in terms of the product of the occupancy probabilities $h_\nu$ for individual pairs,

$$|BCS> = \Pi_\nu((1-h_\nu)^{1/2} + h_\nu^{1/2} a_\nu^+ a_{\bar{\nu}}^+)|0>, \tag{7}$$

where $|0>$ is the fermion vacuum.

Superfluidity is tantamount to the existence of a finite average value of the operators (5), (6) in this state, that is, to a finite value of the order parameter

$$\alpha_0 = < BCS|P^+|BCS > = < BCS|P|BCS >^*, \tag{8}$$

which is equivalent to Cooper pair condensation. In fact, $\alpha_0$ gives a measure of the number of correlated pairs in the BCS ground state. While the pairing gap (4) is an important quantity relating theory with experiment, $\alpha_0$ provides the specific measure of superfluidity. In fact, the matrix elements of the pairing interaction may vanish for specific regions of space, or in the case of specific pairs of time reversal orbits, but this does not necessarily imply a vanishing of the order parameter $\alpha_0$, nor the obliteration of superfluidity.

In keeping with the fact that Cooper pair tunneling is proportional to $|\alpha_0|^2$, this quantity plays also the role of a ($L = 0$) two-nucleon transfer sum rule, sum rule which is essentially exhausted by the superfluid nuclear $|BCS>$ ground state (see Fig. 3). Within the above context, one can posit that two-nucleon transfer reactions are the specific probes of pairing in nuclei.

### B. Fluctuations

The BCS solution of the pairing Hamiltonian was recasted by Bogoliubov [14] and Valatin [15] in terms of quasiparticles,

$$\alpha_\nu^+ = U_\nu a_\nu^+ - V_\nu a_{\bar{\nu}}, \tag{9}$$

linear transformation inducing the rotation in $(a^+, a)$-space which diagonalizes the Hamiltonian (1).

The variational parameters $U_\nu, V_\nu$ appearing in the above relation indicate that $\alpha_\nu^+$ acting on $|0>$ creates a particle in the state $|\nu>$ which is empty with a probability $U_\nu^2 \equiv (1-h_\nu)$, and annihilates a particle in the time reversal state $|\bar{\nu}>$ (creates a hole) which is occupied with probability $V_\nu^2 (\equiv h_\nu)$. Thus,

$$|BCS>= \Pi_{\nu>0}(U_\nu + V_\nu a_\nu^+ a_{\bar{\nu}}^+)|0>, \tag{10}$$

is the quasiparticle vacuum, as $|BCS> \sim \Pi_\nu \alpha_\nu |0>$, the order parameter being

$$\alpha_0 = \sum_{\nu>0} U_\nu V_\nu. \tag{11}$$

Making use of these results we collect in Table 1 the spectroscopic amplitudes associated with the reactions $^{A+2}$Sn(p,t)$^A$ Sn, for $A$ in the interval 112-126, as well as the spectroscopic amplitudes of other pairing modes (see below as well as [16, 17]).

The BCS number and gap equations are,

$$N = 2\sum_{\nu>0} V_\nu^2, \tag{12}$$

$$\frac{1}{G} = \sum_{\nu>0} \frac{1}{2E_\nu}, \tag{13}$$

where

$$V_\nu = \frac{1}{\sqrt{2}}\left(1 - \frac{\epsilon_\nu - \lambda}{\epsilon_\nu}\right)^{1/2}, \tag{14}$$

$$U_\nu = \frac{1}{\sqrt{2}}\left(1 + \frac{\epsilon_\nu - \lambda}{\epsilon_\nu}\right)^{1/2}, \tag{15}$$

while the quasiparticle energy is defined as

$$E_\nu = \sqrt{(\epsilon_\nu - \lambda)^2 + \Delta^2}. \tag{16}$$

### C. Pairing rotations

The phase of the ground state BCS wavefunction may be chosen so that $U_\nu = |U_\nu| = U'_\nu$ is real and $V_\nu = V'_\nu e^{2i\phi}$ ($V'_\nu \equiv |V_\nu|$). Thus [13, 18, 19],

$$|BCS(\phi)>_{\mathcal{K}} = \Pi_{\nu>0}(U'_\nu + V'_\nu e^{-2i\phi} a_\nu^+ a_{\bar{\nu}}^+)|0> = \Pi_{\nu>0}(U'_\nu + V'_\nu a_\nu'^+ a_{\bar{\nu}}'^+)|0> = |BCS(\phi=0)>_{\mathcal{K}'}, \tag{17}$$

where $a_\nu'^+ = e^{-i\phi} a_\nu^+$ and $a_{\bar{\nu}}'^+ = e^{-i\phi} a_{\bar{\nu}}^+$. This is in keeping with the fact that $a_\nu^+$ and $a_{\bar{\nu}}^+$ are single-particle creation operators which under gauge transformations (rotations in the 2D-gauge space of angle $\phi$) induced by the operator $G(\phi) = e^{-i\hat{N}(\phi)}$ and connecting the intrinsic and the laboratory frames of reference $\mathcal{K}$ and $\mathcal{K}'$ respectively, behave according to $a_\nu'^+ = \mathcal{G}(\phi) a_\nu^+ \mathcal{G}^{-1}(\phi) = e^{-i\phi} a_\nu^+$ and $a_{\bar{\nu}}'^+ = \mathcal{G}(\phi) a_{\bar{\nu}}^+ \mathcal{G}^{-1}(\phi) = e^{-i\phi} a_{\bar{\nu}}^+$, a consequence of the fact that $\hat{N}$ is the number operator and that $[\hat{N}, a_\nu^+] = a_\nu^+$.

The fact that the mean field ground state ($|BCS(\phi)>_{\mathcal{K}}$) is a product of operators - one for each pair state - acting on the vacuum, implies that (17) represents an ensemble of ground state wavefunctions averaged over systems with $...N-2, N, N+2...$ even number of particles. In fact, (17) can also be written in the form

$$|BCS>_{\mathcal{K}}=(\Pi_{\nu>0}U'_\nu)\,(1+...+\frac{e^{-(N-2)i\phi}}{(\frac{N-2}{2})!}\left(\sum_{\nu>0}c_\nu a^+_\nu a^+_{\bar{\nu}}\right)^{\frac{N-2}{2}}+\frac{e^{-Ni\phi}}{(\frac{N}{2})!}\left(\sum_{\nu>0}c_\nu a^+_\nu a^+_{\bar{\nu}}\right)^{\frac{N}{2}}$$

$$+\frac{e^{-(N+2)i\phi}}{(\frac{N+2}{2})!}\left(\sum_{\nu>0}c_\nu a^+_\nu a^+_{\bar{\nu}}\right)^{\frac{N+2}{2}}+...)|0\rangle, \tag{18}$$

$_\nu = V'_\nu/U'_\nu$.

sting the Lagrange multiplier $\lambda$ (chemical potential, see Eqs. (12-16)), one can ensure that the mean number ions (Eq. (12)) has the desired value $N_0$. Summing up, the BCS ground state is a wavepacket in the number cles. In other words, it is a deformed state in gauge space defining a privileged orientation in this space, and intrinsic coordinate system $\mathcal{K}'$ [20–22]. The magnitude of this deformation is measured by $\alpha_0$.

### D. Pairing vibrations

he above arguments, point to a static picture of nuclear superfluidity which results from BCS theory. This natural, as one is dealing with a mean field approximation. The situation is radically changed taking into ; the interaction acting among the Cooper pairs (quasiparticles) which has been neglected until now, that is the $G(P^+-\alpha_0)(P-\alpha_0)$ left out in the mean field (BCS) approximation leading to (3) [20, 22]. This interaction entially be written as (for details see e.g. [4] App. J)

$$H_{residual}=H'_p+H''_p, \tag{19}$$

$$H'_p=-\frac{G}{4}\left(\sum_{\nu>0}(U^2_\nu-V^2_\nu)(P^+_\nu+P_\nu)\right)^2, \tag{20}$$

$$H''_p=\frac{G}{4}\left(\sum_{\nu>0}(P^+-P)\right)^2. \tag{21}$$

m $H'_p$ gives rise to vibrations of the pairing gap which (virtually) change particle number in $\pm$ 2 units. The of these pairing vibrations cannot be lower than $2\Delta$. They are, as a rule, little collective, corresponding lly to almost pure two-quasiparticle excitations (see excited $0^+$ states of Fig. 3).

erm $H''_p$ leads to a solution of particular interest, displaying exactly zero energy, thus being degenerate with und state. The associated wavefunction is proportional to the particle number operator and thus to the gauge r inducing an infinitesimal rotation in gauge space. The fluctuations associated with this zero frequency mode , although the Hamiltonian defines a finite inertia. A proper inclusion of these fluctuations (of the orientation in gauge space) restores gauge invariance in the $|BCS(\phi)>_{\mathcal{K}}$ state leading to states with fixed particle number

$$|N_0\rangle\sim\int_0^{2\pi}d\phi e^{iN_0\phi}|BCS(\phi)>_{\mathcal{K}}\sim(\sum_{\nu>0}c_\nu a^+_\nu a^+_{\bar{\nu}})^{N_0/2}|0>. \tag{22}$$

are the members of the pairing rotational band, e.g. the ground states of the superfluid Sn-isotope nuclei. states provide the nuclear embodiment of Schrieffer's ensemble of ground state wavefunctions which is at the the BCS theory of superconductivity.

ning up, while the correlations associated with $H''_p$ lead to divergent fluctuations which eventually restore ry ($[H_{sp}+H''_p,\hat{N}]=0$), $H'_p$ gives essentially rise to non-collective particle number fluctuations, which are

on this point, making use of the so called two-level model, in wihch the single-particle levels associated with occupied (empty) states are assumed to be degenerate and separated by an energy $D$. The parameter which measures the interplay between pairing correlations and shell effects is

$$x = \frac{2G\Omega}{D}, \tag{23}$$

where $G(\approx 25/A$ MeV) is the pairing coupling constant , while $\Omega = (2j+1)/2$ is the pair degeneracy of each of the two levels, assumed to be equal. Making use of the simple estimate of the spacing $D = 2/\rho$ between levels close to the Fermi energy in terms of the level density (for one type of nucleons, e.g. neutrons) $\rho = 3A/2\epsilon_F$ [23], one obtains $D = 4\epsilon_F/3A$ which for $^{120}$Sn leads to $D \sim 0.4MeV$ (cf. e.g. [4] Ch. 2 and refs therein). Making use of the fact that the average pair degeneracy of the valence orbitals of $^{120}$Sn is approximately 3, one obtains $x \approx 3$, implying that pairing effects overwhelm shell effects and the static (pairing rotational) view of Cooper pair condensation is operative.

On the other hand, in a closed shell system like, e.g., $^{208}$Pb, $D \approx 3.4$ MeV. Making use of the fact that the last occupied orbit in $^{206}$Pb is a $p_{1/2}$ orbit, the first unoccupied being a $g_{9/2}$ level, one can use $\Omega = 5$ in calculating the value of $x$, which becomes $x = 0.35$. This value indicates that, in the present case, shell effects are dominant.

This does not mean that Cooper pairs are not present in the ground state of $^{208}$Pb. It means that they break as soon as they are created as virtual states through ground state correlations. Testifying to this scenario is the fact that the expected $2p-2h$ $0^+$ state in $^{208}$Pb at an energy of $2D \approx 6.8$ MeV, is observed at 4.9 MeV. The difference between these two numbers corresponds almost exactly to the sum of the correlation energy of $^{208}$Pb (gs) (0.640 MeV) and of $^{210}$Pb (gs) (1.237 MeV). Thus, the first $0^+$ excited state of $^{208}$Pb corresponds to a two-phonons pairing vibrational state, product of the pair addition ($|^{210}\mathrm{Pb}(gs)\rangle$) and of the pair removal ($|^{206}\mathrm{Pb}(gs)\rangle$) modes of ($|^{208}\mathrm{Pb}(gs)\rangle$).

In other words, we are in presence of an incipient attempt of condensation in terms of two correlated Cooper pairs, which, forced to be separated in two different nuclides by particle conservation, get together in the highly correlated two-phonon pairing vibrational state of $^{208}$Pb. No surprise that its microscopic structure can also be, rather easily, calculated almost exactly, by diagonalizing a schematic pairing force $H_p = -GP^+P$, in the harmonic approximation (RPA). The two-nucleon transfer spectroscopic amplitudes associated with the reactions $^{206}$Pb(t,p)$^{208}$Pb(gs), $^{206}$Pb($^{18}$O,$^{16}$O)$^{208}$Pb(gs), $^{48}$Ca(t,p)$^{50}$Ca(gs), $^{10}$Be(p,t)$^{8}$Be(gs) and $^{9}$Li(p,t)$^{7}$Li(gs), and thus with the excitation (de-excitation) of pair addition and pair subtraction modes, are collected in Table 1. For details, cf. [8].

## III. NUCLEAR FIELD THEORY

Elementary modes of nuclear excitation, namely rotations, vibrations and single-particle motion constitute a choice basis for a compact and economic description of the nuclear structure, as these states incorporate many of the nuclear correlations [3]. The price to be paid for using a correlated basis, is that these modes are non-orthogonal to each other, reflecting the fact that all the nuclear degrees of freedom are already exhausted by the single-particle degrees of freedom. In fact, nuclear elementary modes of excitation are not free, but interact with each other through a coupling term ($H_c$) linear in the single–particle and collective coordinates. Within this (non-orthogonality) context we refer to the similar situation encountered in the case of two-particle transfer reaction mechanism (see above as well as App. A).

A self-consistent field theoretical treatment of this coupling can provide, to each order of perturbation chosen, the solution of the nuclear many-body problem, eliminating in the process overcompleteness and Pauli principle violation of the basis states. Propagating these interactions and corrections to infinite order through the Dyson (Nambu-Gor'kov [24] in the superfluid case) equation, one can carry out a full diagonalization of the many-body problem, provided the rules of the game have been worked out and proved to be right.

A possible answer to such a quest was provided by the Nuclear Field Theory (NFT) [25–31]. With four rules which allow to select the interactions (particle–vibration coupling and four–point vertices $v$), calculate the collective (e.g. RPA for vibrations in spherical, normal nuclei) and the single–particle degrees of freedom (mean field associated with $v$), and eliminate non–allowed processes (diagrams), it was possible to prove that NFT propagators provided the same answer as the Feynman-Goldstone (F-G) many–body propagators to any order of perturbation (cf. App. B). Such a proof is tantamount to the statement that the use of NFT techniques for solving nuclear many-body problems, lead to the correct solution to any given order of perturbation. In particular to the exact solution in the case in which the different contributions are summed to infinite order.

Within this scenario, and provided one has experimental information concerning the collective modes which dress the single-particle states and renormalize the nucleon-nucleon (pairing) interaction, NFT is expected to provide accurate predictions concerning the nuclear structure in general, and two-nucleon spectroscopic amplitudes in particular.

$$G \approx \frac{25}{A}\text{MeV}. \tag{7.25}$$

Making use of this value and of the empirical relation $\Delta = 12/\sqrt{A}$MeV one can write

$$\frac{\Delta^2}{G} \approx 5\text{MeV},$$

or the second term in Eq.(7.18). To be noted that this gain in binding energy, is partially compensated by and increase in single-particle energy associated with the first term and due to the fractional occupation of the single-particle levels around the Fermi surface. The summed effect amounts to only about 1 MeV ($\approx \Delta$) of extra binding energy acquired by the even-even system due to pairing with respect to the odd-even system. This quantity, *which is very important characterize the structure of a nucleus close to the ground state*, is still very small compared to the total binding energy of the system ($\approx A\times 8\text{MeV} \approx 1\text{GeV}$).

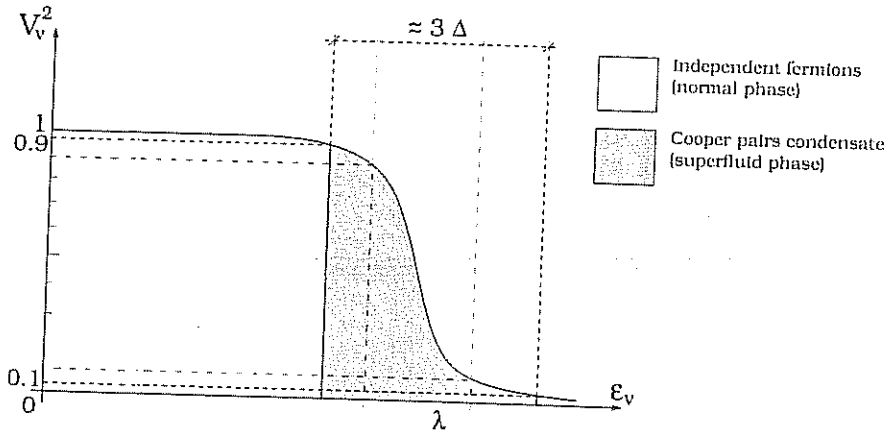


. 7.2. Schematic representation of the occupation of single particles of a non-racting and of a superficial Fermi system, like e.g. nucleons.

n other words, a system of independent particles is affected only on a small ion ($\approx 2\Delta$) around the Fermi energy as compared to this energy ($2\Delta/\lambda = \varepsilon_F \approx 2 - 3\text{MeV}/36\text{MeV} \approx 0.1$). What is actually modified is the occupation he single-particle levels around $\lambda$ (cf. Fig. 7.2). For single-particle states illing $|\varepsilon_\nu - \lambda| \gg 1.5\Delta$, the system retains the single-particle properties*. For

connection with the discussion carried out after Eq. (100), we note that one can produce a rticle-hole excitation based on the states with $|\varepsilon_\nu - \lambda| \gg 1.5\Delta$. Such an excitation would have energy which is at least $3\Delta$, larger than that associated with the breaking of a Cooper pair.

single-particle states such that $|\varepsilon_\nu - \lambda| \lesssim 1.5\Delta$, the occupancy of the levels are strongly modified and the system is composed of nucleons coupled to angular momentum $J = 0$ (singlet states, i.e. $S = 0$ and $L = 0$, $J = L + S$). These pairs are known as Cooper pairs, and behave like bosons (cf. Apps. A and Å, and Fig. 7.3). In nuclei, the number of Cooper pairs is small, typically $4 - 6$ †. One would thus expect strong fluctuations of the associated pairing gap (cf. Ch. 10 and Ch. 13), fluctuations which may blur many of the sharp properties found in the case of infinite systems (bulk matter, thermodynamic limit).

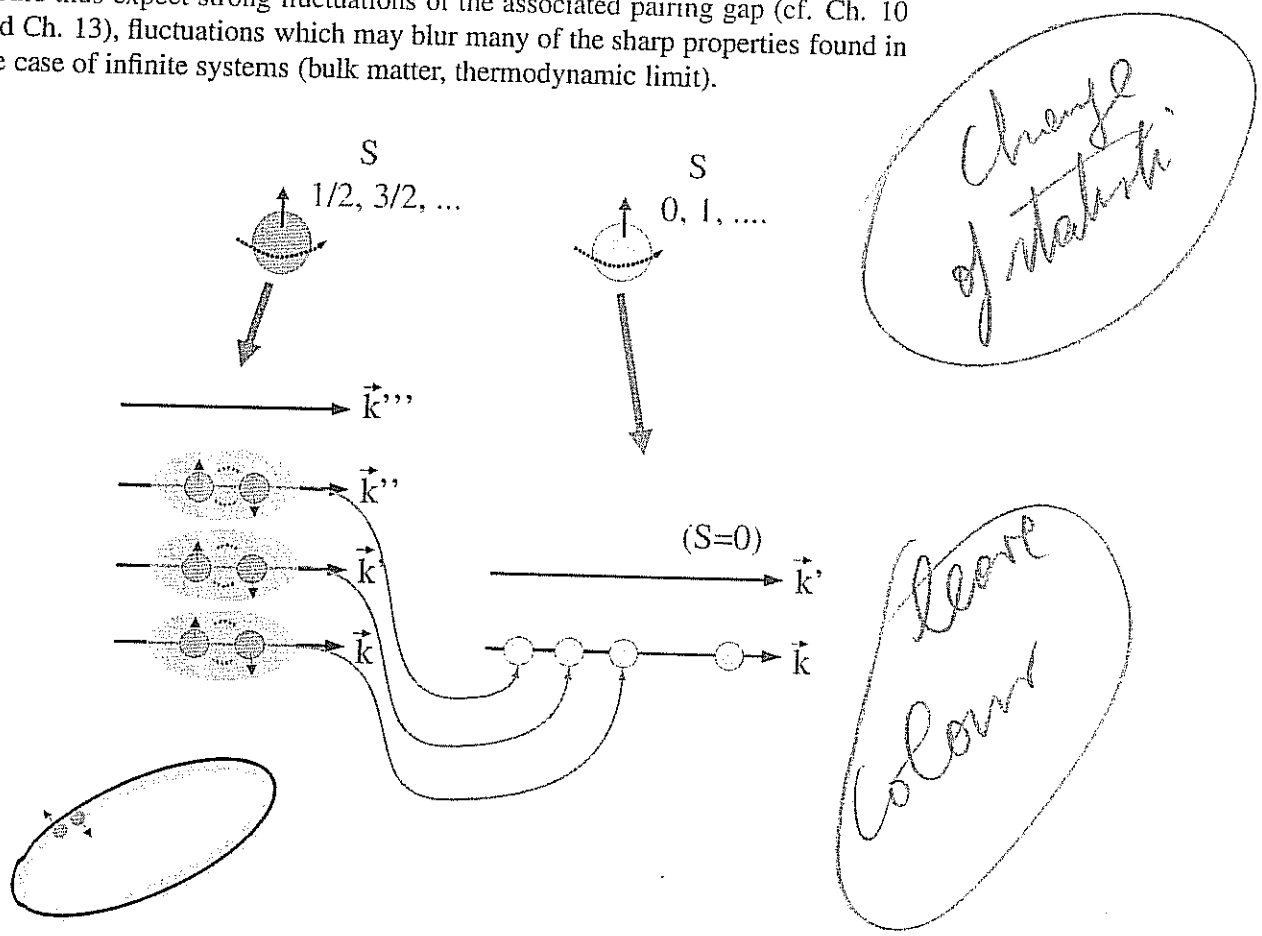


Fig. 7.3. .

Cooper pairs are strongly overlapping and, as befits bosons they occupy the same (lowest energy) state, known also as condensate (cf. Fig. 7.4). The only

† Making use of the BCS solution for a single j-shell, $\Delta = G\Omega/2$, $\Omega = j + 1/2$, for $N = \Omega$ (maximum value of $\Delta$ (cf. Ch. 12)). From the empirical values given in Eqs.(6.2) and (6.6), $\Omega = 2\Delta/G = (24/\sqrt{A}\ \text{MeV})/(25/A\ \text{MeV}) \approx \sqrt{A} \approx 10$ for medium heavy nuclei. Because $N = \Omega = 10$, one concludes that about $\approx 5$ Cooper pairs participate in the nuclear pairing condensation.

way to excite this condensate is by breaking a pair, that is, by providing the

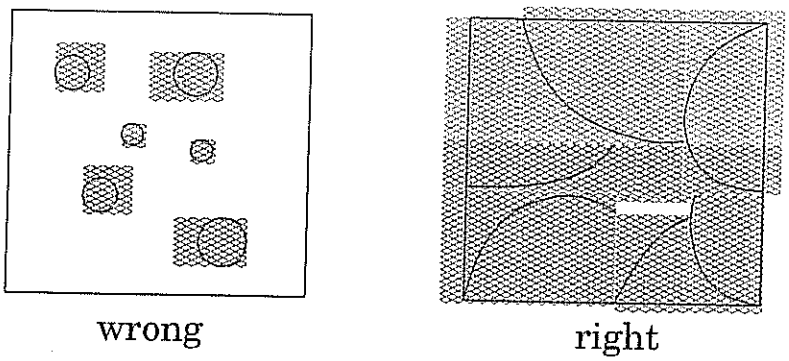


Fig. 7.4. Schematic representation of the distribution of Cooper pairs (close dashed areas) in a superconducting (superfluid made out of fermions) system. To the left we display the so called Schafroth (independent) pair picture. To the right the (right) coherent picture, where Cooper pairs are strongly overlapping.

system with, at least, and energy of $2\Delta$. On the other hand, acting with an external field but providing an energy less than $2\Delta$, the condensed phase will not react, as the first quantal excited state has an energy of at least $2\Delta$.

In particular, if we set a deformed nucleus (cf. Sect. 2.1) into rotation ($\hbar\omega_{rot} < 2\Delta$) one would expect from the above picture the moment of inertia to be about $\frac{1}{2}\mathcal{I}_{\rm rig}$, where $\mathcal{I}_{\rm rig}$ is the rigid (independent particle motion, situation in which the orbitals of the nucleon are strongly anchored to the mean field) moment of inertia. This is because only the matter which is pushed directly by the walls will be set into motion, while the core which should be set into motion by "viscosity" will not react (cf. Fig. 7.5), as the system cannot be excited but by breaking a pair, thus by receiving at least an energy $2\Delta$.

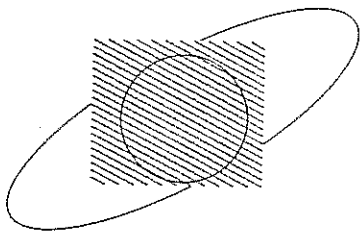

Fig. 7.5. Schematic representation of the reaction to rotation of the superfluid matter filling a deformed nucleus.

From the energy difference between members of a rotational band, which can be accurately parametrized according to the relation (cf. Fig. 2.5)

$$\mathcal{E}_I = \frac{\hbar^2}{2\mathcal{I}} I(I+1), \tag{7.26}$$

one obtains a value of $\mathcal{I}$ which, at low angular momenta, is as predicted by pairing theory, that is, about one half the rigid moment of inertia. In other words, the system can be viewed as a spheroidal container filled with a non-viscous fluid, that is, a superfluid. If one sets the nucleus into rotation, one would then expect to observe a phase transition from the superfluid phase to the normal phase at a rotational frequency in which $\hbar\omega_{rot}$ approximates the value $2\Delta$ needed to break a Cooper pair (cf. Fig. 7.6). In fact, rotational bands have been observed, at very large values of the spin, displaying a rigid moment of inertia.

As we discuss below, the situation is however more subtle than just stated, and is associated with the fact that the nucleus is a zero-dimension superfluid (cf. Chapter 9), displaying strong quantal size effects (QSE), that is, a discrete single-particle spectrum close to the Fermi energy (cf. e.q. Fig. 2.9).

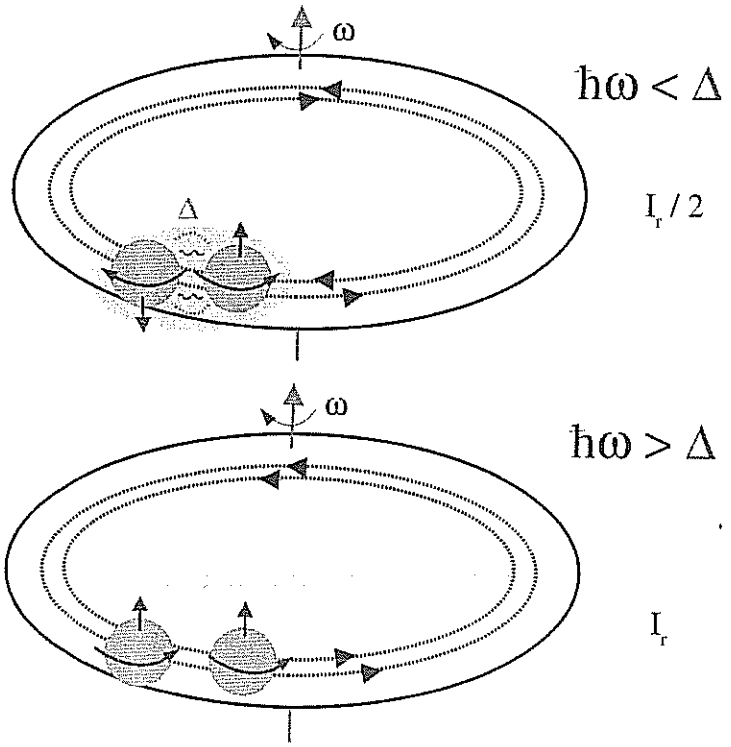


Fig. 7.6. .

# 10

# Symmetry restoration

The term $-G(P^\dagger - \alpha_0)(P - \alpha_0)$ neglected in the mean field BCS treatment of the pairing interaction, contains, aside from constant terms, and terms proportional to the number of quasiparticles of no consequences for the description of levels close to the (zero quasiparticle) ground state, two terms, namely

$$H_p' = -\frac{G}{4}\left(\sum_{\nu>0}(U_\nu^2 - V_\nu^2)(\Gamma_\nu^\dagger + \Gamma_\nu)\right)^2, \tag{10.1}$$

and

$$H_p'' = \frac{G}{4}\left(\sum_{\nu>0}(\Gamma_\nu^\dagger - \Gamma_\nu)\right)^2. \tag{10.2}$$

We shall show that

$$H = H_0 + H_p'', \tag{10.3}$$

where

$$H_0 = \sum_\nu E_\nu N_\nu, \tag{10.4}$$

lead to solutions which conserve the number of particles.

Diagonalizing $H$ in the harmonic (RPA) approximation (cf. App. V)

$$\left[H, \Gamma_{n''}^\dagger\right] = \hbar\omega_{n''}\Gamma_{n''}^\dagger \tag{10.5}$$

$$\Gamma_{n''}^\dagger = \sum_{\nu>0}(a_{n''\nu}\Gamma_\nu^\dagger + b_{n''\nu}\Gamma_\nu), \tag{10.6}$$

one obtains the dispersion relation

$$(\hbar\omega_{n''})^2 \sum_{\nu>0} \frac{1}{((2E_{\nu''})^2 - (\hbar\omega_{n''})^2)\,2E_\nu} = 0, \tag{10.7}$$

and the amplitudes

$$a_{n''\nu} = \frac{\Lambda_{n''}}{2E_\nu - \hbar\omega_{n''}}, \tag{10.8}$$

and

$$b_{n''\nu} = \frac{\Lambda_{n''}}{2E_\nu + \hbar\omega_{n''}}, \tag{10.9}$$

where

$$\Lambda_{n''} = \frac{1}{2}\left[\sum_{\nu>0} \frac{2E_\nu \hbar\omega_{n''}}{((2E_\nu)^2 - (\hbar\omega_{n''})^2)^2}\right]^{-1/2}, \tag{10.10}$$

is the particle-pairing vibration coupling strength.

Eq.(10.7) has as the lowest solution

$$\hbar\omega_{1''} = 0, \tag{10.11}$$

Because we are using a harmonic approximation (cf.Eq.(10.5)), this means that the restoring force of the associated mode is equal to zero. Thus, we are dealing with a deformation.

The state $|1''\rangle$ is then given by the expression

$$\begin{aligned} |1''\rangle &= \Gamma^\dagger_{1''}|o''\rangle = \lim_{\hbar\omega_{n''}\to 0} \sum_{\nu>0} (a_{n''\nu}\Gamma^\dagger_\nu + b_{n''\nu}\Gamma_\nu)|o''\rangle \\ &= \lim_{\hbar\omega_{1''}\to 0} \Lambda_{1''} \sum_{\nu>0} (\Gamma^\dagger_\nu + \Gamma_\nu)|o''\rangle \\ &= \lim_{\hbar\omega_{1''}\to 0} \frac{\Lambda_{1''}}{2\Delta}\hat{N}|o''\rangle = \lim_{\hbar\omega_{1''}\to 0} \sqrt{\frac{\hbar^2}{2\mathcal{D}_{1''}\hbar\omega_{1''}}}\hat{\alpha}|o''\rangle, \end{aligned} \tag{10.12}$$

where

$$\hat{\alpha} = \lim_{\hbar\omega_{1''}\to 0} \sqrt{\frac{\hbar^2}{2D_{1''}\hbar\omega_{1''}}}(\Gamma^\dagger_\alpha + \Gamma_\alpha). \tag{10.13}$$

in keeping witht the fact that we are calculating a one phonon state.

Expression (10.12) indicates that the lowest one-phonon state is obtained fromt he vacuum state by a rotation in gauge space, thus implying that $|o''\rangle$ ($\sim |BCS\rangle$) defines a privileged direction in space. On the other hand, Eq.(10.13)

implies that the fluctuations in this orientation diverge, as the zero point fluctuations $(\hbar^2/2\mathcal{D}_{1''}\hbar\omega_{1''})^{1/2}$ go to infinity as the frequency goes to zero. In other words, the system rotates in gauge space, thus recovering gauge invariance (conservation of particle number, cf. Eq.(11.11)). From the relation

$$\frac{\Lambda_{1''}}{2\Delta} = \sqrt{\frac{\hbar^2}{2D_{1''}\hbar\omega_{1''}}}, \tag{10.14}$$

one obtains the inertia of the collective mode (rotation in gauge space)

$$\frac{D_{1''}}{\hbar^2} = 4\sum_{\nu>0}\frac{U_\nu^2 V_\nu^2}{E_\nu} = \sum_{\nu}\frac{|\langle\nu\bar{\nu}|\hat{N}|0\rangle|^2}{2E_\nu}, \tag{10.15}$$

which is the cranking formula for the moment of inertia. In the case of a single $j$-shell

$$\frac{D_{1''}}{\hbar^2} = \frac{4N}{G\Omega}\left(1-\frac{N}{2\Omega}\right) \tag{10.16}$$

which, for $N = \Omega$ becomes

$$\frac{D_{1''}}{\hbar^2} = \frac{2}{G}, \tag{10.17}$$

a quantity which coincides with $\mathcal{I}/\hbar^2$ (cf. Eq.(12.8)).

Note that for small values of $N$ (making the ansatz that $N$ is a continuous variable), the relation between $E_0$ and $N$ is linear (cf. Eq.(12.7)) indicating a boson dispersion relation. In fact, associated with the phenomenon of spontaneous symmetry breaking of particle number conservation, one has a Anderson-Goldstone-Nambu [27-29] (cf. also [30]) mode, which eventually shows up as a pairing rotational band, as $N$ can have only finite values and thus the quadratic term in Eq.(12.7) overwhelms the linear dependence.

If one were to diagonalize the full Hamiltonian $H_0 + H'_p + H_{p''}$ one would again obtain a root at zero frequency, aside from pairing vibrations, i.e. linear combinations of two-quasiparticle states, associated with fluctuations of the pairing gap. These pairing vibrations have always energies $\geq 2\Delta$, and are not particularly collective in superfluid nuclei, becoming very collective in normal nuclei around closed shells.

On the other hand, these fluctuations have important consequences in the pairing phase transition, that is the way the pairing gap goes to zero as a function of e.g. rotational frequency. In fact, the pairing gap for the solution which conserve particle number can be written as (cf. Fig. 10.1)

$$\Delta = \sqrt{\Delta_{\mathrm{BCS}}^2 + \Delta_{\mathrm{RPA}}^2}, \tag{10.18}$$

where

$$\Delta^2_{\mathrm{RPA}} = \sum_n \langle 0|P|n\rangle\langle n|P^+|0\rangle, \tag{10.19}$$

$|n\rangle$ being the pairing vibrational states, solutions of $[H + H'_p + H_p'', \Gamma^\dagger_n] = \hbar\omega_n \Gamma^\dagger_n$, where one excludes from the summation the Anderson-Goldstone-Nambu mode ($\hbar\omega_1 = 0$).

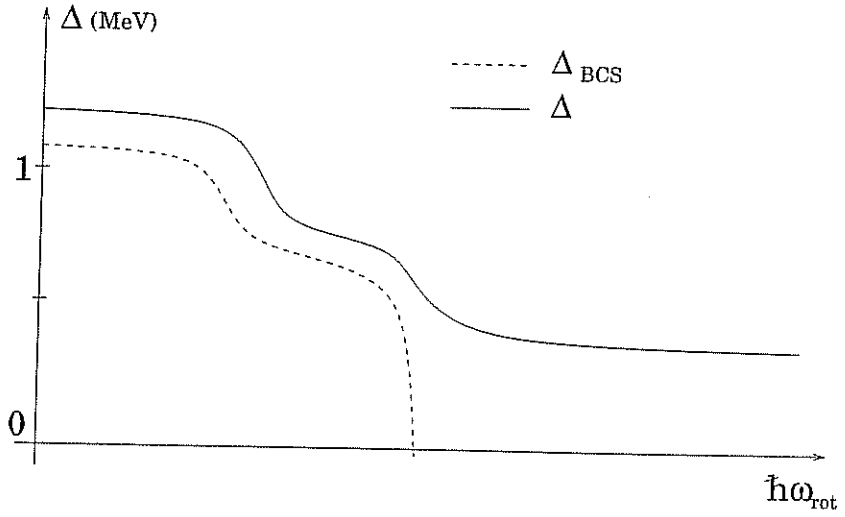


Fig. 10.1. .

This behaviour cannot be measured directly, but its consequences can be observed in e.g. the variation of the moment of inertia as a function of the rotational frequency. From Fig. 10.1 one expects $\mathcal{I}$ to rise from the superfluid value to the rigid value, with kinks at each band crossing. This, in fact, is what the experimental data seems to indicate (cf. Fig. 9.3).

# 11

## Origin of the pairing interaction

App M.